UNIVERSITY OF CRETE
DEPARTMENT OF MEDICINE
POSTGRADUATE PROGRAMME: MOLECULAR BASIS OF HUMAN DISEASE
COMMITTEE:PR. KARDASSIS D., SAVVAKIS C., TALIANIDIS I.

The role of Usp22 de-ubiquitinase in the regulation of metabolic and carcinogenesis pathways.

Master Diploma Thesis: Stiliani Baliou

Athens, AL. Fleming 2014

Table of Contents

Abstract

USP22 is a thiol-specific protease that can remove ubiquitin from ubiquitinated histones H2A and H2B. USP22 has been recently identified as a member of the 11-gene cancer stem cell signature proposed to serve as a predictor of treatment resistance, tumor aggressiveness and metastatic potential of human cancers. Studies in yeast indicate a critical role for Usp22 in transcriptional initiation and elongation. However, its role in mammals remains elusive. We aimed to address the role of Usp22 in the mouse liver. Our work focuses on the role of Usp22 in metabolic regulation, cell cycle progression and hepatocarcinogenesis. Preliminary results using wild-type mice under conditions of fasting indicated increased levels of Usp22 compared to normally fed controls. Additionally, when mice were subjected to partial hepatectomy increased levels of Usp22 were observed. Consistent with a potential role of Usp22 in cell proliferation, analysis of livers from mice bearing experimentally induced tumors also indicated upregulation of Usp22, compared to normal age-matched livers. In all cases, Usp22 displayed nuclear localization, similar to untreated livers, as assessed by immunohistochemical analysis. Our results indicate a putative involvement of Usp22 in metabolic regulation and in cell cycle progression in murine liver. We are currently in the process of generating three genetic models that will be useful for studies aimed at understanding Usp22 function in liver. The first one is an Usp22 conditional liver-specific knock-out mouse, the second is a transgenic mouse overexpressing human USP22 upon tamoxifen treatment and the third one is a transgenic mouse overexpressing a catalytically inactive C185S mutant form of human USP22. Phenotypic characterization, genome wide expression and occupancy analysis of these models will be useful towards elucidating the role of Usp22 and the dynamics of histone ubiquitination in the mammalian liver.

I. Introduction

1.1.1. The structure of chromatin

Within the eukaryotic cell nucleus, genetic information is organized in a highly conserved structural polymer, termed chromatin, which supports and controls the crucial functions of the genome. The chromatin template undergoes dynamic changes during many genetic processes. These include necessary structural reorganizations that occur during DNA replication and cell cycle progression, spatially and temporally coordinated gene expression, as well as DNA repair and recombination events.

Historically, chromatin has been classified as either euchromatic or heterochromatic. Euchromatin is decondensed chromatin, although it may be transcriptionally active or inactive. Euchromatin is implicated in different processes including DNA replication, transcription and replication-relative processes. Heterochromatin can broadly be defined as highly compacted. It may exist as permanently silent chromatin (constitutive heterochromatin), where genes are rarely expressed in any cell type of the organism or repressed (facultative heterochromatin) in some cells during a specific cell cycle or developmental stage. Heterochromatin is condensed, transcriptionally inactive and associated with repressive histone modifications, whereas euchromatin is relatively accessible and associated with actively transcribed genes and active histone modifications (Goldknopf *et al*. 1975).

1.1.2. Epigenetic regulation of chromatin structure

The transcriptionally active chromatin regions contain nucleosomes, but in an “unfolded state”, they still impose an obstacle to the transcription machinery. Some transcription factors, whether they are activators or suppressors, can gain access to their sites contained in nucleosomes, but others cannot. Moreover, the machinery recruited by the DNA-bound regulators and responsible for delivering RNA pol II to promoters is obstructed by the presence of nucleosomes.

A number of distinct mechanisms serve to reconfigure the chromatin, poising genes for subsequent transcription, promoting initiation or elongation. The first mechanism refers to

the use of ATP-dependent chromatin remodeling complexes capable of mobilizing nucleosomes and altering the structure of nucleosomes. These complexes can be categorized into two representative families: SNF2H (or ISW1 and ISW2 in yeast) and Brahma-Swi/Snf family (Flaus and Owen–Hughes. 2004; Narlikar *et al.* 2002; Peterson. 2002). The second mechanism involved in gene activation is a selective octamer loss at promoters. The third major mechanism involved in setting up transcriptional states is the presence of histone variants (Mito *et al.* 2005; Zhang *et al.* 2005). The fourth mechanism refers to the post-translational modifications in histone tails, which are thought to be involved in various chromatin-dependent processes including transcription.

1.1.3. Post translational modifications of histones

The nucleosome is the fundamental repeating unit of chromatin (Konberg. 1974). The basic chromatin unit is composed of a protein octamer containing two molecules of each canonical (or core) histone (H2A, H2B, H3 and H4), around which is wrapped 147 bp of DNA. (Luger *et al.* 1997; Khorasanizadeh. 2004). Based on amino acid sequence, histone proteins are highly conserved from yeast to humans and are composed from a globular domain and flexible (relatively unstructured) “histone tail” which protrudes from the surface of the nucleosome. These tails are subjected to several post-translational modifications, which regulate the chromatin structure and function during diverse biological processes such as DNA replication, gene regulation, DNA repair and chromosome condensation (Henikoff. 2005).

Reversible post-translational modifications (PTMs) at core histones influence the nature of the chromatin landscape. Histone PTMs occur at specific amino acids on histone tails including methylation (Me), acetylation (Ac), propionylation (Pr), butyrylation (Bu), crotonylation (Cr), 2-hydroxyisobutyrylation (Hib), malonylation (Ma), succinylation (Su), formylation (Fo), ubiquitination (Ub), citrullination (Cit), phosphorylation (Ph), sumoylation (SUMO) and hydroxylation (OH) (Dawson *et al.* 2012; Huang *et al.* 2014; Kouzarides. 2007; Marquardt and Thorgersson. 2014). All the post-translational modifications in chromatin structure are tightly associated with function.

Modified histones participate in key cellular processes, dictating the accessibility of chromatin to factors that drive gene transcription and proteins that function in DNA repair pathways. Along with DNA methylation, histones PTMs are major components of the epigenome and may become dysregulated during tumorigenesis.

1.1.4. Ubiquitination of histones

Ubiquitin is a highly conserved 76 amino acid long peptide that can be covalently conjugated to lysine residues of eventually every protein in a multi-step enzymatic process.

Depending on the number of ubiquitin moieties that are attached to the substrate, the proteins can be mono-ubiquitinated or poly-ubiquitinated. In the first case of mono-ubiquitination, a single ubiquitin moiety is attached to one or several lysine residues on the substrate which in turn regulates processes ranging from membrane transport to transcription (Sigismund *et al.* 2004). On the other hand, the proteins are modified by polyubiquitination, in which a chain of more than four ubiquitin moieties are attached to one of seven lysine residues (Haglund *et al.* 2005). The most-studied polyubiquitin chain is linked to lysine (K48) and usually marks a protein for degradation in the proteasome (figure 1).

Histone H2A was the first protein shown to be ubiquitinated (Goldknopf *et al.* 1975) and its ubiquitination site was further mapped to be the highly conserved Lys119 residue (Nickel and Davie. 1989). The majority of H2A appears to be mono-ubiquitinated; however, it can exist in a poly-ubiquitinated form in several cell types and tissues (Nickel *et al.* 1987). In addition to H2A, H2B was also found to be ubiquitinated (West & Bonner. 1980) and although H2B is less abundant than H2A, it appears to be conserved from yeast to human. In contrast to H2A, only a mono-ubiquitinated form of H2B has been reported (Thorne *et al.* 1987).

Mono-ubiquitination of histones is associated with transcriptional control of gene expression and the DNA damage response. Furthermore, cleavage of this single ubiquitin from histones H2A and H2B has been associated with chromatin condensation prior to packaging of DNA into chromosomes.

The effects of mono-ubiquitination on each core histone can vary and can be either activating or repressive. H2B mono-ubiquitination is catalyzed by Rad6/Bre1 (Kim *et al.* 2005; Wood *et al.* 2003; Zhu *et al.* 2005) and is correlated to the active transcription in combination with H3K4 methylation (Henry *et al.* 2003; Kao *et al.* 2004). It has also been shown that H2B ubiquitination is required for genome stability through stabilizing fork progression at replicative strands (Trujillo and Osley. 2012). Additionally, H2B ubiquitination orchestrates the appropriate chromatin landscape in order to overcome RNA Pol II stalling (Mao *et al.* 2014). On the other hand, the ubiquitination of H2AK119 is mediated by enzyme Bmi/Ring1A and is associated with transcriptional repression as well as silent chromatin states (Wang *et al.* 2006). This change, however, is not conserved in yeast (Wang *et al.* 2004; Wang *et al.* 2006).

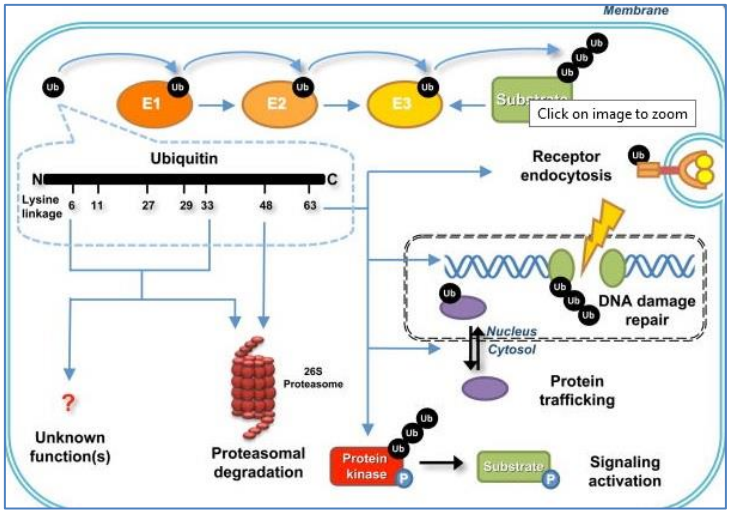

Figure 1: Ubiquitination regulates protein degradation or activation. Ubiquitination reaction involves three enzymes. The K48-linked ubiquitination is directed to the 26S proteasome for protein degradation. In contrast, the K63-linked ubiquitination regulates signaling activation involved in distinct biological functions such as receptor endocytosis, DNA damage repair, protein trafficking, and signaling activation (Yang *et al.* 2010).

1.1.5. Enzymes involved in histone ubiquitination and deubiquitination

Ubiquitination is a highly dynamic post-translational modification that plays a regulatory role in virtually every cellular process. Ubiquitin is a 76 amino acid long peptide that can be covalently conjugated to lysine residues of proteins in a multi-step enzymatic process involving the sequential action of an ubiquitin activating enzyme (E1), an ubiquitin conjugating enzyme (E2) and an ubiquitin ligase (E3). In humans, two E1 enzymes (Uba1 and

Uba6), approximately 30 E2s and more than 600 E3 ligases have been identified (Komander *et al.* 2012). In a few cases, nonlysine residues have been reported as ubiquitination targets, such as cysteine, threonine and serine (Ciechanover *et al.* 1998; Wang et al. 2007).

Although ubiquitination of all proteins uses the same E1 enzyme, the action of E2 and especially E3-ligase enzymes appears to be substrate specific (Pickart *et al.* 2001). In the case of histone H2B , the yeast Rad6 and Bre1 (and their human homologues) appear to share the E2 and E3 ligase actively (Hwang *et al.* 2003; Jentsch *et al.* 1987; Koken *et al.* 1991; Wood *et al.* 2003) and are capable of ubiquitinating histones *in vitro* (Koken *et al.* 1991) and *in vivo* (Hwang *et al.* 2003). In contrast to H2B, the physiological E2 and E3 enzymes that catalyze the ubiquitination of histone H2A have not yet been identified.

As mentioned before, ubiquitination is a reversible modification and deubiquitinating enzymes (DUBs) catalyze the removal of Ub from targeted substrates. DUBs are thiol proteases that cleave the isopeptide bond at the carboxy-terminal-most Gly76 residue of Ub, either removing Ub from the substrate or processing the poly-ub chain. The defining characteristic of UBPs is the presence of conserved domains, called the Cys-box and His-box, which are involved in formation of a "catalytic triad" for proteolytic cleavage and are reminiscent of the papain family of cysteine proteases.

The human genome encodes around 100 enzymes that catalyze the removal of Ub from targeted substrates. These DUBS are classified in 5 major superfamilies: 1) the Ubiquitin-specific proteases superfamily (USPs), Usp1-Usp46, 2) the ovarian tumor (OTUs) superfamily (OTUB1,OTUB2), 3) the Machado-Josephin Domain (MJD) superfamily (ATXN3,ATXN3L), 4) ubiquitin C-terminal hydrolases (UCH) superfamily (BAP1, UCHL1,UCHL3,UCHL5), (Nijman *et al.*2005b) 5) The Jab1/Mov34/Mpr1 Pad1 N-terminal^{+} (MPN^{+}) (JAMM) domain superfamily. In contrast to the first four superfamilies, which are cysteine proteases, the proteins consisting the fifth family can bind zing finger domain and they are metalloproteases.

In addition to housekeeping functions associated with the recycling and metabolism of ubiquitin, DUBs can also act to spare proteins from degradation or to modulate their function (Komander *et al.* 2009; Nijman *et al.* 2005; Reyes-Turcu *et al.* 2009).

1.1.6. The structure of Usp22

The human USP22 gene is located on chromosome 17 and consists of 14 exons whereas mouse Usp22 is located on mouse chromosome 11 and consists of 13 exons. Four (4) Usp22 isoforms have been identified in human but only one in the mouse genome (figure 2).

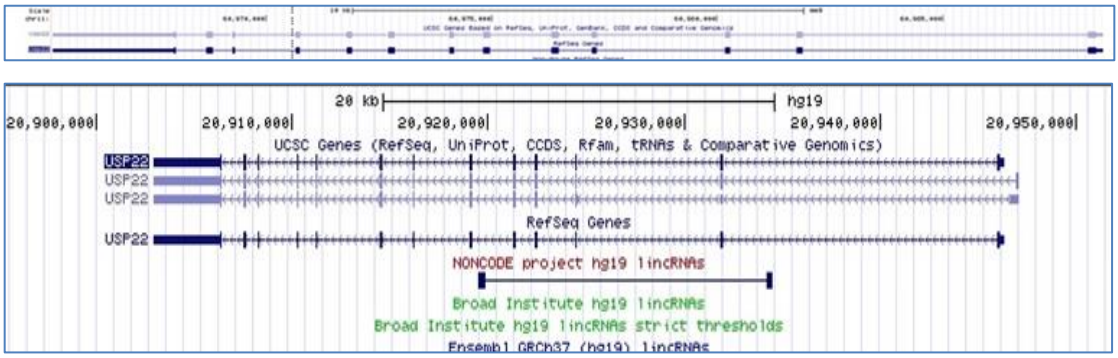

Figure 2: Mouse isoform and human isoforms of Usp22.

USP22 is a member of deubiquitinating enzyme family. It contains a carboxy-terminal ubiquitin domain that exerts hydrolase activity (Lee *et al.* 2006). In addition, USP22 contains an amino-terminal zinc finger domain that may mediate its interaction with other proteins (Ingvarsdottir *et al.* 2005), (figure 3).

Although USP22 contains highly conserved Cys, Asp (I), His, and Asn/Asp (II) domains characteristic of ubiquitin-specific processing proteases, the fact that shows low protein homology to other known USP proteins, such as USP2, USP7 and USP36 (Lee *et al.* 2006), indicates that USP22 may function in a specialized manner in the DUB family.

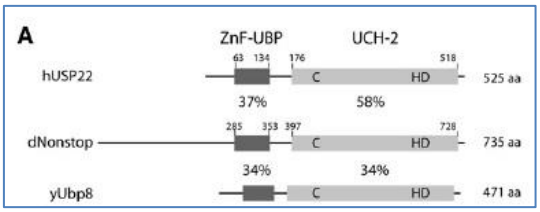

Figure 3: Schematic representation of Ubp8 orthologs in human (hUSP22), Drosophila (dNonstop), and S. cerevisiae (yUbp8). Sequence identities in the N-terminal zinc finger domain (ZnF-UBP, dark gray) and in the C-terminal catalytic site (UCH-2, light gray) are indicated relative to the human USP22 sequence (Zhao *et al.* 2008).

1.1.7. The physiological role of Usp22

Usp22 appears to be essential for mouse embryogenesis and Usp22 deficient embryos were detected dead 10.5 days after post implantation stage (Lin *et al.* 2012). It has been demonstrated that Usp22 is a deubiquitinase of Sirt1 and leads to suppression of p53 transcriptional activity and p53-mediated cell apoptosis, through Sirt1 stabilization, both during embryonic development and in response to DNA damage (Lin *et al.* 2012).

USP22 is a component of the SAGA multi-subunit complex and has been demonstrated that its full activity requires the interaction with other partners of SAGA (Lang *et al.* 2011). The SAGA complex plays an important role in triggering specifically the transcription of cellular stress responsive genes (Huisinga and Pugh. 2004).

The importance of USP22 during development was first reported by Weake and his colleagues using Drosophila melanogaster as a model system. Their study revealed that different SAGA components, especially Nonstop (homolog of USP22 in Drosophila) play an important role in neuronal development by driving accurate axon guidance in the optic lobe (Weake *et al.* 2008). Moreover, it was reported that the phenomenon position-effect variegation was dependent on the activity of Nonstop (homolog of USP22 in drosophila) and of dSgf11 (homolog of ATXN7L3/interacting partner of USP22 at SAGA in drosophila), (Zhao *et al.* 2008).

In addition to its role in development, USP22 appears to be strongly associated with pathological conditions like cancer, highlighting its role in cell cycle progression, proliferation and DNA-replication related processes.

1.1.8. USP22 as member of SAGA transcriptional co-activator complex

Usp22 is a component of SAGA multi-subunit complex. The yeast SAGA (Spt-Ada-Gcn5-acetyltransferase) complex is a 1.8-MDa complex and is composed of 19 or more protein subunits which are highly conserved in eukaryotes (Baker *et al.* 2007; Grant *et al.* 1997; Lee *et al.* 2007). It has been mentioned that under normal conditions, SAGA can sustain overall H2Bub distribution in genomic regions irrespective of their transcriptional status compared to results obtained from SAGA inactivation (Lang *et al.* 2011). However, retention of SAGA at gene promoters was observed at the subset of SAGA-dependent genes, such as stress-

induced genes (Huisinga and Pugh. 2004; Lang *et al.* 2011). Recently, additional data have demonstrated that this complex has an important role in promoting gene expression because it mediates its activity as a general co-activator complex required for the transcription of all Pol II genes at both their promoters and their transcribed regions (Bonnet *et al.* 2014).

The yeast SAGA complex (figure 4) consists of structural modules that can function as distinct units including 1) a recruitment module (Tra1), (Grant *et al.* 1998) 2) an acetylation module (Gcn5, Ada2, and Ada3), (Balasubramanian *et al.* 2002), 3) a TBP interaction unit (Spt3 and Spt8) (Bhaumik et al. 2004; Sterner et al. 1999), 4) a DUB module (Ubp8, Sus1, Sgf11, and Sgf73), (Daniel *et al.* 2004; Henry *et al.* 2003; Lee *et al.* 2005 ; Shukla *et al.* 2006; Rodriguez-Navarro *et al.* 2004) and 5) an architectural unit (Spt7, Spt20, Ada1, TAF5, TAF6, TAF9, and TAF12), (Grant *et al.* 1997; Grant *et al.* 1998).

Based on its acetylation and deubiquitination modules, the SAGA complex can mediate multiple activities and functions as transcriptional activator (Baker *et al.* 2007; Nagy *et al.* 2007; Rodriguez-Navarro. 2009). The HAT and DUB activities within this complex are carried out by Gcn5 and Ubp8 (yeast homolog of Usp22), respectively. These modules interact with other SAGA subunits in order to form a HAT module containing Gcn5/GCN5 together with Ada2/ADA2b, Ada3/ADA3, and Sgf29/SGF29 (Grant *et al.* 1997) and a DUB module composed of Ubp8/USP22, Sgf73/ATXN7, Sgf11/ATXN7L3, and Sus1/ENY2 (Rodriguez-Navarro. 2009).

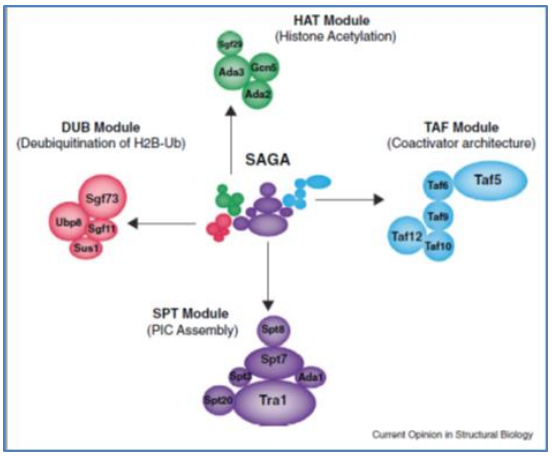

Figure 4: The composition of SAGA (Samara and Wolberger. 2011)

The full assembly of the given modules is crucial to enhance the substrate recognition and specificity of yGcn5/hGCN5 as well as to increase the ubiquitin protease activity of the

complex (Clements *et al.* 2003; Kohler *et al.* 2010; Lang *et al.* 2011; Samara *et al.* 2010). It is of particular interest that the stability of SAGA complex is affected by the loss of deubiquitinase or acetylatransferase activity, whereas its integrity is not. Altogether, these data point to a strong conservation throughout evolution not only of the SAGA protein composition but also of its modularity.

Actually, Ubp8 (yeast homolog of Usp22) has to be incorporated within the histone acetyltransferase SAGA complex and its DUB activity requires assembly with regulatory factors forming a tetrameric deubiquitinating module (Ingvasdottir *et al.* 2005; Kohler *et al.* 2010; Lee *et al.* 2005; Samara *et al.* 2010). Similarly, USP22 has been shown to be active *in vitro* only when it interacts with all subunits of the DUB module, including ATXN7L3. It has also been found to be fully active *in vivo* only as a part of the SAGA complex (Armour *et al.* 2013; Lang *et al.* 2011).

In yeast, Sus1, Sgf11 and Ubp8 form a structural entity within the SAGA holoenzyme and the association of the Dub module with the rest of the complex is mediated by Sgf73 (Ingvarsdottir *et al.* 2005; Kohler *et al.* 2010). The complex is organized in two functionally distinct parts encompassing two different domains of Ubp8. The first part is referred as "assembly lobe" and is characterized by a dense packing of all four subunits that are extensively contacting each other. The second one is mentioned as the "catalytic lobe" and Ubp8 subunit is surrounded by hydrophobic interaction of the catalytic triad (Cys-146, His-427, and Asn-443) and of the C2H2-like zinc finger domain (ZnF) of Sgf11 (Greenblatt *et al.* 2005; Samara *et al.* 2010). More recent evidence indicated that the Zn-F domain of Sgf11 can be sufficient to cause the conformational changes that allow the catalytic active residues of DUB to be exposed (figure 5). Using deletion assays of Sgf11-Znf, it was found that Sgf11 plays a role in organizing the active site rather than in promoting binding of the substrate ubiquitin (Kohler *et al.* 2010). The Sgf11-ZnF domain was shown to play an unexpected role in maintaining the catalytic activity of Ubp8 by ensuring the proper organization and folding of the four-protein complex (Samara and Wolberger. 2012).

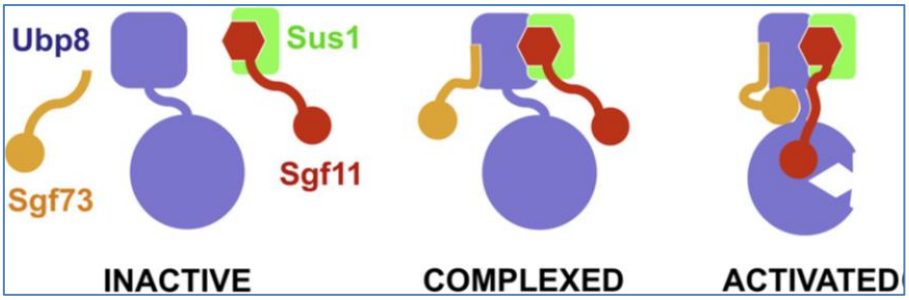

Figure 5: Model for the Assembly and Activation of the SAGA DUB Module Free Ubp8 (blue) has a ZnF-UBP domain (square) and an inactive catalytic domain (full circle). Independent from other subunits, Sus1 (green) can form a complex with Sgf11 (red) by wrapping around its N-terminal helix (hexagon). The correctly positioned ZnF domains of Sgf11 (red circle) and Sgf73 (orange circle) are both required to fully activate Ubp8 (sharp teeth) (Koehler *et al.* 2014).

Lastly, it could be mentioned that other components of SAGA which are not involved in DUB sub module can interfere with this. For instance, ySus1 is present in two functionally different protein complexes, the ySAGA complex where it regulates its deubiquitination activity through interactions with yUbp8 and ySgf11 and the TREX/AMEX complex, where it plays a role in mRNA export (Kohler *et al.* 2006; Kurshakova *et al.* 2007; Oliver *et al.* 2012; Parscual-Garcia *et al.* 2008).

1.1.9. The substrates of Usp22

The known USP22 substrates include both histone and non-histone substrates. Concerning histones, the potential importance of Usp22 to deubiquitinate both H2Aub and H2Bub has been highlighted recently (Zhang *et al.* 2008; Zhao *et al.* 2008). Concerning non-histone substrates, it has been proposed that this protein can promote stability of multiple cancer-associated protein targets through deubiquitination of TRF1 (Atanassov *et al.* 2009), of BMI1 (Liu *et al.* 2010) and of SIRT1 (Lin *et al.* 2012) thus affecting oncogene accumulation. It is noteworthy that USP22 is likely to recycle TRF1 by deubiquitination, making it available for reincorporation into telomeres. This function may be one of the reasons why Usp22 is overexpressed in rapidly proliferating cancer cells (Glinsky *et al.* 2006). Additionally, it has been demonstrated that Usp22 can contribute to 3'-end processing of JAK-STAT-inducible mRNAs and so it can be used as a cancer stem cell marker (Chipumuro and Henriksen. 2012). Lastly, concerning its correlation with stem cell signature, it has been found that USP22 can be the driving force for lineage-specific differentiation programmes occupying Sox2 locus and inhibiting its transcription (Sussman *et al.* 2013).

Lastly, it is significant to evaluate the interaction of Usp22 with Sirt1 (a key player in metabolism) separately (figure 6). The interaction between Sirt1 and Usp22 has been examined extensively, producing contradictory results. In one publication, whole body loss of Usp22 in mice was closely correlated to the increase in p53 transcriptional activity and apoptotic function, when cells face DNA damage, through instability of Sirt1 (Lin *et al.* 2012). In the second publication, it has been shown that this interaction facilitates recruitment of Sirt1 deacetylase activity to the DUBm/SAGA complex which in turn has a regulatory effect in SAGA acetylation and complex formation. As a result, researchers supported the view that acetylation at single lysine K129 of Usp22 was sufficient to change the association of the protein with SAGA complex. In that case, the interaction of Usp22 with SIRT1 did not stimulate Usp22 activity. Contrary to previous reports, a noticeable effect was not observed because of the loss of Usp22 activity on either of the steady-state levels or deacetylase activity of SIRT1 (Armour *et al.* 2013). The third study claimed that Usp22-Sirt1 interaction was the intermediate step for inhibiting Stat3 signaling pathways (Ao *et al.* 2014). In the same direction, the fourth study provided the first insights into the negative transcriptional regulation of Usp22 by classical deacetylase inhibitors (Xiong *et al.* 2014).

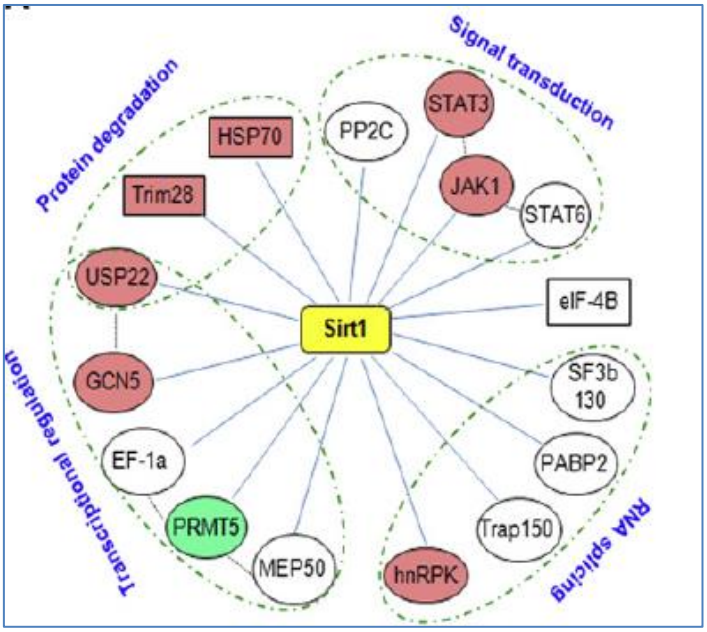

Figure 6: **Interaction network of Sirt1-associated proteins**. Red: the proteins were confirmed to interact with Sirt1 by coimmunoprecipitation and western blotting. Green: protein interaction could not be confirmed. White: not tested (Lin *et al*. 2012).

1.1.10. The role of Usp22 in carcinogenesis

Recent studies have shown that DUBs play major roles in normal physiological processes and their aberrant activity seems to be responsible for diseases including cancer (Clague *et al.* 2012; Cole *et al.* 2014; Colland *et al.* 2010; Jacq *et al.* 2013; Nijman *et al.* 2005; Singhal *et al.* 2008; Sowa *et al.* 2009). As far as cancer progression is concerned, recent studies highlighted the potential importance of USP22, which can deubiquitinate both H2Aub and H2ABub (Zhang *et al.* 2008; Zhao *et al.* 2008).

A large body of research linked the human USP22 with tumor progression and oncogenic activity in order to be used in therapeutic interventions. According to Glinsky, human USP22 was identified as part of an 11-gene signature termed the "Death-from-Cancer" signature that predicts rapid disease recurrence, distant metastatic sites and poor response to therapy across multiple solid tumors (Glinsky *et al.* 2005). Remarkably, the predictive power of the 11-gene stem cell signature remains high even when assessing early stage cancer patients and when examined tumors were derived from a variety of epithelial and non-epithelial cell types. This signature includes the Bmi1 polycomb group protein and several Bmi1 target genes, suggesting that this molecular signature is related to stem cell-like characteristics (Berezovska *et al.* 2006). Human Usp22 was shown to act as an oncogene (Liu *et al.* 2011), regulating cell cycle progression, proliferation and apoptosis (Atanassov *et al.* 2011). Consistent with that, enrichment was shown to act as a key indicator of poor prognosis in a variety of different cancers including invasive breast cancer (Zhang *et al.* 2011b), colorectal carcinoma (Liu *et al.* 2011), esophageal cancer (Li *et al.* 2012), papillary thyroid carcinoma (Wang *et al.* 2013), gastric cancer (Yang *et al.* 2011), oral squamous cell carcinoma (Piao *et al.* 2012), salivary duct carcinoma (Dai *et al*. 2014; Piao *et al.* 2013), non-small cell lung carcinoma (Ning *et al.* 2012), cervical cancer (Yang *et al.* 2014) and brain glioma (Li *et al.* 2013; Liang *et al*. 2014). In hepatocellular carcinoma (HCC) (Ling *et al.* 2012) and bladder cancer (Lv *et al.* 2011), the loss of USP22 was indicated to arrest the cell cycle and suppress proliferation rate.

Importantly, studies regarding USP22 expression in tumors showed that USP22 protein expression and its nuclear accumulation were correlated exponentially to unfavorable prognosis in different human cancer types (Kapoor. 2013; Xiong *et al.* 2014; Zhang *et al.*

2011). As it was expected, higher levels of USP22 in tumors facilitating the progression of tumor and metastatic structures were found.

Initially, a significant role of USP22 was reported in ligand-induced androgen receptor (AR)-mediated transactivation, in both *Drosophila* and human cells (Zhao *et al.* 2008), which may at least partially explain its oncogenic properties. (Dubik *et al.* 1987; Gurel *et al.* 2008; Riggins *et al.* 2007; Wolfer *et al.* 2010). Additionally, in multiple xenograft models of human cancer, it has been demonstrated that Usp22 controls androgen receptor (AR) accumulation and signaling. The result was the enrichment of target genes which were regulated by androgen receptor and finally led to prostate cancer (Schrecengost *et al.* 2014). Among the targets that were regulated transcriptionally by USP22 were the Myc onco-protein and other sequence-specific activators that require hSAGA activity, including p21, cyclin D2, and CAD (Zhang *et al.* 2008).

1.1.11. Usp22 and metabolism

There is no direct link between Usp22 and metabolism; however there are several hints that can provide grounds to study the role of Usp22 in metabolism. It is generally known that SAGA appears to promote the transcription of genes that respond to environmental stress such as heat, DNA damage and metabolic starvation. It is noteworthy that USP22 is required for the transactivation of nuclear receptors such as androgen receptor, estrogen receptor and glucocorticoid receptor (Zhao *et al.* 2008), proposing a possible link of Usp22 with hepatic nuclear receptors tightly associated with metabolism. Furthermore, it has been demonstrated that USP22 interacts strongly with SIRT1 (a key player in metabolism- figure 7), suggesting that Usp22 may be regulated by metabolic fluctuations through its association.

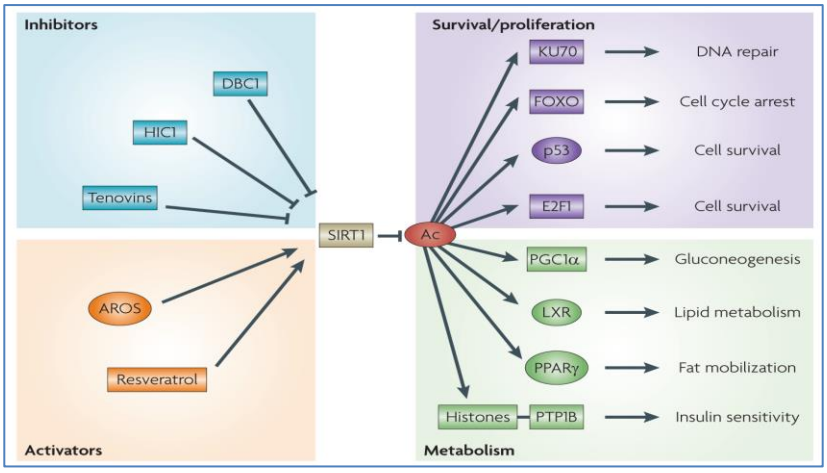

Figure 7: SIRT1 is an NAD^+-dependent histone deacetylase that catalyzes the removal of acetyl (Ac) groups from a number of non-histone targets and its following consequences are detected in lipid metabolism, insulin sensitivity, reverse cholesterol transport and gluconeogenesis as well as cell survival and senescence effects (cell survival and DNA repair). Several protein regulators and small-molecule compounds that can activate or inhibit SIRT1 function have also been described. AROS, active regulator of SIRT1; DBC1, deleted in breast cancer 1; FOXO, forkhead box; HIC1, hyper methylated in cancer 1; LXR, liver X receptor; PGc1α, PPARγ coactivator 1α; PPARγ, peroxisome proliferator-activated receptor-γ; PTP1B, protein-tyrosine phosphatase 1B (Brooks and Gu. 2009).

SIRT1 (silent mating type information regulator 2 homolog 1) the mammalian ortholog of yeast Sir2, is a highly conserved NAD^+-dependent protein deacetylase that has gained major attention due to its ability to sense metabolic status with adaptive transcriptional outputs (Lomb *et al.* 2010). In general, SIRT1 functions as a molecular switch adapted to metabolic fluctuations (Chen *et al.* 2008; Hagopian *et al.* 2003), which regulates the expression of a number of genes involved in diverse signaling pathways such as gluconeogenesis in the liver, fat mobilization in white adipose tissue and insulin secretion in the pancreas.

SIRT1 has been suggested to mediate the transcription of peroxisome proliferator-activated receptor γ coactivator-1α (PGC-1a) which determines the mitochondrial biogenesis in skeletal muscle during food deprivation (Cerutti *et al.* 2014; Gerhart-Hines *et al.* 2011; Price *et al.* 2012; Rodgers *et al.* 2005). Considering the dependence of Sirt1 on cellular NAD^+, the Sirt1 levels can be increased by AMPK activation. So, it has been proposed that the AMPK-mediated phosphorylation of PGC-1α serves as a priming signal for the subsequent PGC-1α deacetylation which is induced by AMPK through boosting intracellular NAD^+ levels (Canto *et al.* 2012). The question remains how AMPK activation leads to an increase in intracellular NAD^+ levels. In contrast, there is a compelling evidence that SIRT1 is upregulated firstly, leading to the increase of AMPK substrate, LKB1 (Hou *et al.* 2008; Ivanov *et al.* 2008; Lan *et al.* 2008).

It is significant that whole-body SIRT1 knockout mice are protected from high-fat diet-induced obesity and fatty liver (Canto *et al.* 2012; Schenk *et al.* 2013). Using liver-specific knockout mice (SIRT1 LKO), it was shown that SIRT1 functions as marker required for induction and maintenance of fatty acid oxidation in response to low glucose concentrations impairing PPARα signaling and inhibiting fatty acid β-oxidation (Bai *et al.* 2011; Gehart-Hines *et al.* 2011). Walker *et al.* and Ponugoti *et al.* recently showed that SIRT1 may also regulate hepatic lipid metabolism (figure 8) through deacetylation of SREBPs (Ponugoti *et al.* 2010; Walker *et al.* 2010), critical regulators of lipogenesis and cholesterol genesis (Guarantee.2006; Osborne *et al.* 2009). In addition, SIRT1 is involved in the regulation of cholesterol metabolism through deacetylation of LXRs (Li *et al.* 2007; Purushotham *et al.* 2009) which are capable of regulating the reverse cholesterol transport and suppressing the intestinal cholesterol uptake (Feige *et al.* 2007). Finally, SIRT1 deacetylates and increases transactivation potential of farnesoid X receptor (FXR) which indirectly represses hepatic fatty acid (FA) and triglyceride (TG) synthesis. Deacetylation of FXR leads to increased heterodimerization with Retinoid X receptor (RXRa) and DNA binding, though it decreases FXR stability (Kemper *et al.* 2009).

Alternatively, it was demonstrated that the pharmacological induction of SIRT1 by resveratrol resulted in PPAR-γ-mediated transcriptional repression and subsequently inhibition of adipogenesis (Picard *et al.* 2004; Tontonoz *et al.* 2008).

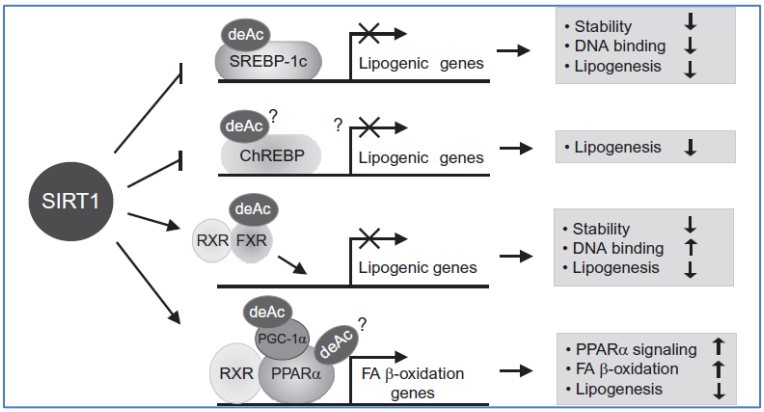

Figure 8: **Regulation of hepatic fat (TG) metabolism by SIRT1**. During fasting, SIRT1 affects the activity of metabolic regulators involved in transcriptional programs of hepatic lipogenesis and b-oxidation. First, SIRT1 deacetylates SREBP-1c and thereby, inhibits hepatic lipogenesis program and at the same time induces the b-oxidation process through PPARa signaling. Alternatively, SIRT1 is required for transactivation of FXR which is known to indirectly repress hepatic FA and TG synthesis (Kemper *et al.* 2013)

II Aims

Usp22 is a subunit of the human SAGA transcriptional co-factor acetylation complex and as a member of this complex, functions to deubiquitinate histone H2B (Zhang *et al.* 2008). The association of expression of Usp22 with stem cell-like features in many cancers and deubiquitination of histone H2B may result in reversion to a non-differentiated phenotype. We hypothesize that the histone deubiquitinase, Usp22, is important for hepatic gene expression and cell cycle progression.

Preliminary data in the lab suggested that Usp22 may be the major histone deubiquitinase in hepatocytes. The specific aims of my project are

1. ***Generation of animal models lacking or overexpressing Usp22.***
2. ***Studying the role of Usp22 in normal conditions during liver development and in conditions of experimentally induced cancer and in metabolic conditions.***

II. Materials and Methods

1. Animals

Mice with Usp22 cassette are available in the lab. These mice are being crossed with either *Alfp-Cre* or *Alb-Cre or TTR-Cre-ERT* mice to obtain hepatocyte-specific inactivation of the *Usp22* gene in embryonic and adult liver, respectively.

2. DNA extraction from mouse tails

Approximately 1cm of mouse tails was incubated with 500µl tail buffer containing 200 µg Proteinase K, at 55 ^{o}C overnight. The tail buffer was composed of 50 mM Tris, pH=8.0, 400 mM NaCl, 100 mM EDTA and 0, 5% SDS.

The next day, a volume of 25:24:1 (v/v/v) phenol/chloroform/isoamyl alcohol (Sigma) was added to each tube containing the mouse tail. The tubes were vortexed vigorously for 10 seconds and micro centrifuged for 10 minutes at 13.000 rpm at room temperature (RT). The upper aqueous phase was carefully removed and transferred to a new clear eppendorf tube.

Then, equal volume of 24:1 (v/v) chloroform/isoamyl alcohol was added to the upper aqueous phase in order to remove any traces of remaining phenol. The process was continued by centrifuging the samples again for 30 seconds at 13.000 rpm at room temperature (RT). The aqueous phase was carefully removed and transferred to a new eppendorf tube. Equal volume of isopropanol was then added and the tubes were mixed well by shaking them (without pipetting) till a white precipitate appeared. That precipitate, corresponding to the DNA, was then isolated-"fished out" with a glass Pasteur Pipette, then washed by immersing it in 1ml of 70% (v/v) ethanol and let to dry at room temperature (RT). Finally, DNA was dissolved in an appropriate volume of ultra-pure DNase free water and stored at -20 ^{o}C.

2. Generation of human USP22 and human mutant C185S USP22 plasmid constructs.

Full-length human USP22 was isolated from Flag-pcDNA3 vector (sent from Tora L. lab) and was amplified by polymerase chain reaction (PCR). The primers used for PCR amplification were the following: 1) forward primer with BamH1 restriction site: 5'-AGGATCCATGGTGTCCCGGCCAGAGCCC G-3' and reverse primer with Xho1 restriction site: 5'-AGAATTCCTACTCGTATTCCAGGAACTG-3'.

The amplified DNA fragment was gel extracted and cloned into pCMV-3HA vector which was previously digested with BamH1 and XhoI. All the digestions were performed sequentially and according to each enzyme's optimal conditions. The colonies were selected with diagnostic digestions if they had the insert and the construct isolated from the positive ones was sequenced. After verification, the pCMV-3HA-human USP22 containing plasmid was digested with XhoI1 and Not1 and sub cloned into the pEF1a-(36/37)-hER1 (LBD) 847bp1781bp (G400V/M543A/L544A with ligand binding domain) vector. This lately step was performed in order to create an Usp22 fusion protein which contains an LBD at the N-terminus which will modulate the expression of Usp22 in a tamoxifen induced manner. The 3HA-hUsp22-LBD construct is sub cloned into the TTR vector in order to finally create an induced HA tagged USP22 construct which serves to generate the Usp22 transgenic mice (procedure in process). Respectively, we amplified the mutated USP22 fragment and inserted it into the BamH1/XhoI digested pCMV-3HA-LBD vector. The primer pairs which were used for amplification of the mutated gene consisted of the forward primer with BamH1 site: 5'-GC-GGA TCC-GTG-TCC-CGG-CCA-GAC-CCC-GAC-GGC-3' and the reverse primer with XhoI1 site: 5'- GC-CTG-GAG-CTC-GTA-TTC-CAG-GAA-TTT-GTG-3'. In combination with the above primers, the following primer pair was used which contained the forward primer: 5'- CTT-GGG-AAC-ACA-AGC-TTC-ATG-AAC-3' and the reverse primer: 5'- GTT-CAT-GAA-GCT-TGT-GTT-CCC-AAG-3' in order to substitute cysteine 185 to serine.

3. Genotyping via PCR amplification

Approximately, 200 ng of tail DNA was used as template to be amplified in Polymerase Chain reaction (PCR). The DNAs were used as template in qPCR reaction containing dNTPs 10 mM,

10X Taq buffer (500 mM KCl, 100 mM Tris-HCl pH=8.5, 15 mM $MgCl_2$, 1% Triton X-100), $MgCl_2$ 25 mM , Taq Polymerase, Betain 5M and the specific primers for Usp22 gene. The steps of the PCR procedure were: step of denaturation at 94°C for 3 minutes followed by 30 cycles of denaturation at 94°C for 1 minute, annealing at 58°C for 1 minute and extension at 72°C for 1 minute. Finally, samples were maintained at 72°C for 10 minutes in order to be extended. The details of the genotyping primers used are mentioned below.

Additionally, we used Flp pair of primers: forward primer :5'-GAG-AAG-AAC-GGC-ATA-GTG-CG-3' and reverse primer: 5'-GAC-AAG-CGT-TAG-TAG-GCA-CAT-3'. Respectively, we used Cre pair of primers: forward primer: 5' AGG-TGT-AGA-GAA-GGC-ACT-CAG-C-3' and reverse primer 5'-CTA-ATC-CGC-CAT-TCT-TCC-AGC-AGG-3'.

Assay	5' Forward Name	5' Forward Sequence	3' Reverse Name	3' Reverse Sequence	Product size
LacZ	LacZ_2_small_F	ATCACGACGCGCTGTATC	LacZ_2_small_R	ACATCGGGCAAATAATATCG	108bp

Assay	5' Forward	5' Forward Sequence	3' Reverse	3' Reverse Sequence	Product Size
FRT	5FRT_F	AGGCGCATAACGATACCACGAT	5FRT_R	CCACAACGGGTTCTTCTGTT	204bp

Assay	5' Forward Name	5' Forward Sequence	3' Reverse Name	3' Reverse Sequence	Product size
Usp22	Usp22 (1)_F and wt F	C GAACTTCGGAATAGGAACTTCG GACCCACCATGCTACAAAA	Usp22(1)_R	ACCACAGCCGTCCTTAACC	145bp(wt)/267bp (mutated band with Usp22)

Assay	5' Forward Name	5' Forward Sequence	3' Reverse Name	3' Reverse Sequence	Product size
Usp22	Usp22 (2)_loxp_F	GTC CTT GTG AAA CTG AAC TC	Usp22(1)_loxp_R	CCC ACC ACT GCA TGT AAC AG	186 bp

Table of primer sequences for genotyping of Usp22 cassette.

4. Immunofluorescence assay

Approximately 1cm in diameter, the liver sample was immersed in an OCT embedding compound, containing tissue mold and let to freeze onto a specialized metal grid, which was placed in liquid nitrogen containing cabinet-box. 5 µm in thickness sections were obtained in the cryostat at -23 °C and mounted on special histological slides (Super frost Plus, VWR). The sections were either air-dried at room temperature (RT) and directly used for immunofluorescence or stored intact at -80 °C for later use and analysis. For immunofluorescence, the tissue sections were fixed for 10 minutes at room temperature (RT) with 4% formaldehyde in PBS (formalin) and permeabilized with 0, 2 % PBS-Triton-X100 for 10 minutes at room temperature (RT). Then the sections were blocked with 5% BSA/ 0.1% Triton-X100 for 1 hour at room temperature (RT) and incubated with primary antibody against Usp22 at 4 °C overnight. Next day, the sections were washed 3 times with PBS (10 minutes each) and incubated with Alexa Fluor® 488 conjugated secondary

antibody at room temperature for one more hour. The nuclei were stained with DAPI and the stained cells of the tissue were observed under an Inverted Fluorescence Microscope using laser filters set for FITC and DAPI.

4. Nuclear and whole cell extract preparation from cell lines

Nuclear extracts

Tissue culture cells were collected, washed, and gently resuspended by pipetting in hypotonic buffer A (25 mM Hepes (pH 7.9), 1.5 mM MgCl2, 10 mM KCl, 0.1% NP40, 1 mM DTT, 0.5 mM PMSF, 10 μg/ml Approtinin) in order to prepare nuclear extracts. Correct Lysis was observed with Trypan blue. Intact nuclei were then centrifuged for 5 minutes at 3000 rpm at 4°C. The supernatant cytoplasmic fraction was removed and a volume of 100 μλ of Buffer A was added again (without disturbing the pellet) in order to remove any remaining traces of the cytoplasmic fraction. Samples were centrifuged again for 1minute at 3000 rpm at 4 °C and supernatant was discarded. An equal volume of high salt Nuclear Lysis Buffer NLB800 (25 mM Hepes (pH 7.9), 10% Glycerol, 0.8 M KCl, 0.2 mM EDTA (pH 8.0), 0.1% NP40, 1 mM DTT, 0.5 mM PMSF, 10 μg/ml Approtinin) was added to the samples and the process continued with rotation of the samples at 4°C for 30 minutes. After the extraction, the nuclei were centrifuged at 14.000 rpm at 4°C for 15 minutes and the nuclear extract supernatant fraction was transferred to a new prechilled Eppendorf tube and stored at -80 ^{o}C. The concentration was determined by Bradford assay.

Whole Cell extracts

Tissue culture cells were collected, washed and suspended in SDS-free RIPA buffer (50 mM Tris-HCl (pH 7.5), 1% NP40, 0.25% Na-Deoxycholate, 150 mM NaCl, 1 mM EDTA (pH 8.0), 10% Glycerol, 1 mM PMSF, 2 μg/ml Approtinin) in order to prepare whole cell extracts. The samples were rotated at 4 °C for 20 minutes in order to be lysed. Then, we centrifuged the samples immediately at 14.000 rpm at 4 °C for 20 minutes, collected their supernatant containing the soluble proteins in new prechilled tubes and stored them at -80°C.

An alternative protocol based on SDS and sonication was used in order to extract the insoluble proteins. In that case, 2x SDS Laemli Buffer was directly added to the pellet. The

crucial step of this extraction was the 5-minute sonication (Diagenode Bioruptor) in order to extract the insoluble protein fraction.

6. 2/3 Partial hepatectomy

Partial hepatectomy was performed following the protocol published in Nature Protocol (Mitchell and Willenbring. 2008). Eight week-old male mice (weighing 20–25 grams) underwent 2/3 PH under inhalational isofluorane anesthesia (anesthetic machine Matrx), (13 per genotype per time point). Isoflurane is an inhalant anesthetic that is widely used in veterinary medicine because of its safety and rapid recovery of the animal after surgery, and it is considered the anesthetic of choice for 2/3 PH surgeries (Faller *et al.* 2012; Panzer *et al.* 2009; Suliburk *et al.* 2005). 2/3 PH consisted of a midline laparotomy with removal of the left and anterior (median) liver lobes and the gallbladder. Surgeries were performed between 7 and 11:30 p.m. Mice rapidly regained consciousness and had immediate access to food and water. The development of small areas of hepatocyte necrosis was not observed in any mouse of each genotype. Liver tissue was either immersed in fixative (Formalin) or snap-frozen frozen (OCT Embedding Medium) and stored at −80°C.

7. Preparation of protein extracts from animal tissue and western blot analysis

Liver (or/and other tissue) extracts were prepared by homogenizing an approximately 0,8 mm in diameter tissue piece in 1 ml SDS free RIPA Buffer (50 mM Tris pH=7.5, 1% NP40, 0.25% Na-Deoxycholate, 150 mM NaCl, 1mM EDTA, 10% Glycerol and protease inhibitor coctail (Roche)) using the Polytron tissue homogenizer at 20000 stroke setting. Immediately after homogenization, rotating samples were incubated at 4 °C for 20 minutes for the lysis to proceed. Samples were then centrifuged at 14.000 rpm 4 °C for 20 minutes and their clear lysate was then transferred to prechilled new tubes and stored immediately at -80 °C. The concentration of the total protein was determined by Bradford assay.

Equivalent amounts of total protein (50 μg) from each sample were separated by SDS-PAGE electrophoresis, and then transferred onto a nitrocellulose membrane which was previously immersed in methanol. Appropriate transfer of the proteins was determined by Ponceau Staining. The membrane was blocked with PBS containing 0.1% Tween-20 and 5% nonfat milk at room temperature (RT) for 1 hour while it was being shaken gently. The blocking solution was then removed and the membrane was incubated with the specific

primary antibody diluted in PBS containing 0.1% Tween-20 and 5% nonfat milk specific at 4°C overnight. The following steps were three repetitive washes with PBS containing 0.1% Tween-20 (PBST) which lasted 10 minutes. The process continued with incubation of the membrane with the corresponding secondary antibody. The membrane was washed with PBST 3 times (each time for 10 minutes) and then specific protein bands were detected using the ECL Advanced Western Blot detection Kit. The densitometry analysis of bands was performed using the Image J programme.

The used primary antibodies were Usp22 (C-3) mouse monoclonal antibody (Av) raised against amino acids 130-176 of Usp22 of human origin (Santa Cruz Biotechnology-sc390585) in different dilutions (1:200, 1:500, and 1:1000) and mouse monoclonal Gcn5 primary antibody (Santa Cruz Biotechnology) with respective secondary antibody-goat anti-mouse HRP in 1:5000 dilution (Santa Cruz Biotechnology). Primary anti - b-tubulin rabbit Ab 1:2000 dilution (Abcam) was used as endogenous loading control. The specificity of Usp22 antibody was verified by Western blot analysis using T293 cell extracts transfected with human Usp22.

8. RNA extraction- Real time PCR

The RNA was chemically purified by the Trizol method. Specifically, 0. 5 mm in diameter tissue was immersed in 1 ml of Trizol and homogenized with Polytron for 20 seconds. After homogenization, the samples were incubated at room temperature (RT) for 5 minutes. A volume of 200μl RNAase-free chloroform was added to each tube and samples were vortexed immediately and incubated at room temperature (RT) for 3 minutes. Then, samples were centrifuged at 12.000 rcf at 4^{o}C for 15 minutes so that the insoluble material (extracellular membranes, polysaccharides, and high molecular weight DNA) could be removed. The aqueous phase was transferred to new eppendorf tubes and RNA was then precipitated with two volumes of 100% ethanol and 1/10 volume sodium acetate pH=5.2 at -20^{o}C overnight. Next day, the samples were micro centrifuged at 14.000 rpm at 4^{o}C for 30 minutes and RNA pellet was washed twice with 70% alcohol. After being centrifuged for 5 minutes at 14.000 rpm 4^{o}C, the pellets were dried with speedvac (Dynap-Vap/Labnet) and then dissolved in an appropriate volume of ultra-pure RNAase free water.

Equal volume of 25:24:1 (v/v/v) phenol/chloroform/isoamyl alcohol (Sigma) was added to each tube. The tubes were vortexed vigorously for 20 seconds and microcentrifuged at

14.000 rpm at 4°C for 15 minutes. The upper aqueous phase was carefully removed and transferred to a new clear eppendorf tube.

In order to remove any traces of the remaining phenol, equal volume of 24:1 (v/v) chloroform/isoamyl alcohol was added to the previously upper-aqueous phase and the tubes were vortexed and centrifuged again at 14.000 rpm at 4°C for 15 minutes. RNA was then precipitated overnight with 2 volumes of 100% ethanol with 1/10 volume sodium acetate pH=5.2. The next day, the samples were micro centrifuged at 14.000 rpm at 4°C for 30 minutes and white precipitates corresponding to RNA were dissolved in an appropriate volume of ultra-pure DNAase free water and stored at -20 °C. According to Dnase I kit, total RNAs were treated with 10 U of DNase I (Invitrogen) at 37°C for 30 minutes. Before and after Dnase treatment, 1 μg RNA from each of our samples was electrophorized in a 2% agarose gel at 90 Volt constant. In this way, the quality and quantity of the RNA could be assessed. The picture of three bands corresponding to 28s, 18s and 5s RNA was shown with the first band to be more intense, which was the desirable result. In case there was contamination with DNA, a smear above the RNA bands could be detected.

For cDNA synthesis, 1 μg of RNA was used as template in a reaction which included dNTPs 10 mM, oligo dTs 100 ng/μl and 5xRT buffer (Invitrogen). After vortexing and spinning the samples, the reactions were incubated at 65 °C for 5 minutes, cooled at room temperature for 10 minutes and then SuperScript reverse transcriptase (RT; Invitrogen) was added. The reactions were incubated at 37 °C for 1 hour and cDNAs were stored in -20°C.

The cDNAs were diluted 1:20 and 4 μλ of the diluted sample was used as template in qPCR reaction containing dNTPs 10 mM, SyberGreen, $MgCl_2$ 25 mM , Taq Polymerase, Betain 5M and the specific primers. Thermo cycler conditions included an initial holding at 95 degrees for 10 minutes, which was followed by a two-step PCR programme: 95 degrees for 15 seconds, 60 degrees for 20 seconds for 45 cycles and 72 degrees for 15 seconds. The programme finished with a melting-curve stage: 50 degrees for 1 minute and 95 degrees for 15 seconds. Data were collected and quantitatively analyzed on an detection system (Applied Biosystems). The mean value of the replicates of each sample was calculated and expressed as cycle threshold (C_t cycle number at which each PCR reached a predetermined fluorescence threshold, set within the linear range of all reactions). The amount of gene expression was then calculated as the difference (ΔC_t) between the mean C_t value of the sample for the target gene and the mean C_t value of that sample of the endogenous control

(GAPDH). Relative expression of genes was expressed as $2^{-\Delta\Delta CT}$ over ΔCt of control sample. The Real time- PCR primer pairs were the following: Usp22 forward primer: 5'-GTG-GGC-TCC AGT-CTG-ATG-TTA-C-3' and Usp22 reverse: 5'-GAA-TGG-GGT-AGA–AGA-ACC-GGG-A-3'. Gapdh forward primer: 5'-CCA-ATG-TGT-CCG-TCG-TGG-ATC-T-3' and Gapdh reverse primer: 5'-GTT-GAA-GTC-GCA-GGA-GAC-AAC-C-3'.

9. Statistical Analysis

Prism 6 (GraphPad Prism) was used to graph all noted data. Results are expressed as mean values + SD. P values were calculated by two-sided independent t-test, and a p value, 0.05 was considered significant.

Results Part A

Generation of Animal Models

IV. Results Part A

Generation of animal models: An Introduction

All the acquired knowledge on Usp22 function has come from experiments conducted on cultured cell lines, given that whole body Usp22 depletion seems to be embryonic lethal. Specifically, Usp22 deficient embryos were detected dead 10.5 days after post implantation stage (Lin *et al.* 2012). In order to study Usp22 function in vivo, conditional knock-out Usp22 mice were needed to be generated. More specifically, we focused on the generation of liver-specific Usp22-KO mice and transgenic mice overexpressing either the wild type human or a human mutant form of Usp22.

Liver is an ideal organ to study the role of Usp22 in cancer and metabolism. Usp22 is expressed in mouse liver and appears to be enriched in several types of cancer including hepatocellular carcinoma, as indicated by studies using cells lines, such as HepG2 cells. Another advantage of liver that renders it as a good model for this study is its enormous capacity to regenerate, that gives us the opportunity to monitor the cell cycle progression *in vivo* by partial hepatectomy. Finally, liver is a good model both for developmental studies in embryos (differentiating and proliferating hepatoblasts) and adults (fully differentiated hepatocytes in resting Go phase) and for highly reproducible biochemical studies since it comprises a homogenous organ of a single cell type.

1. Generation of conditional knock-out mice

In order to produce conditional knock-out mice, the following technique was used in which a selected gene becomes disrupted in a specific tissue at a certain time of its development. This strategy takes advantage of a site-specific recombination system to excise- and thus disable- the target gene in a particular place or at a particular time. The most common of these recombination systems, called Cre/lox, is widely used to engineer gene replacements.

Mice with the Usp22 cassette described in figure 9 are available in the lab. This cassette contains a floxed exon2 of Usp22, an Frt-neo cassette containing also the lacZ gene which encodes b-galactosidase. Initially, we crossed these mice with mice overexpressing Flp recombinase in order to delete the Frt-neo cassette. The Frt-neo cassette contains a splice acceptor site which acts as a gene trap cassette and would lead if no removed by the Flp recombinase to the generation of full knock-out mice which we know from literature that is embryonic lethal (Lin *et al.* 2012).

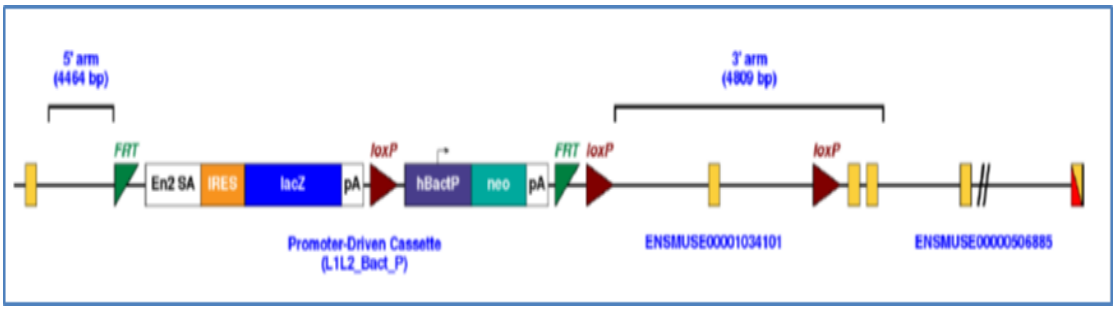

Figure 9: The Usp22 cassette with floxed exon 2 of Usp22 (provided by EUCOMM) which is used for the production of different conditional knock-out mice.

The resultant progeny still contained the cassette of Usp22 but no longer expressed Neo or LacZ as a result of the deletion of the region flanked by the FRT sites. In our case, the target gene is replaced by another version of the gene, in which exon 2 is flanked by a pair of the short DNA sequences, called Loxp sites, that are recognized by the Cre recombinase protein and homologous recombination is performed.

We have initiated breeding of floxed Usp22 mice with Alfp-Cre transgenic mice to obtain hepatocyte-specific inactivation of Usp22 in embryonic stages. Currently, we have pairs of Usp22lox/wt–Alfp-Cre heterozygous mice in breeding to obtain homozygous Usp22-deficient mice.

We have initiated breeding of floxed Usp22 mice with Alb-Cre transgenic mice to obtain hepatocyte-specific inactivation of Usp22 in postnatal stages. Currently, we have pairs of Usp22lox/wt – Alb-Cre heterozygous mice in breeding to obtain homozygous Usp22-deficient mice.

We have initiated breeding of floxed Usp22 mice with TTR-CreERT transgenic mice to obtain hepatocyte-specific Tamoxifen inducible inactivation of Usp22. Currently, we have pairs of Usp22lox/wt – TTR-CreERT heterozygous mice in breeding to obtain homozygous Usp22-deficient mice.

Polymerase Chain Reaction (PCR) was used to genotype the mice and detect the population that carried the desired cassette. We examined the presence of the mutant allele by using three different sets of primers which normally did not anneal in the murine genome. The first set of primers was designed to detect the LacZ sequence of Usp22 cassette. The second set was designed against the Frt sequence of Usp22 cassette (figure 10b). The third set was gene specific (termed Usp22 (1)), which was designed not only to detect the presence of the mutant allele but also to discriminate the wild type versus heterozygous and homozygous mice at later stages (figure 10b). After the action of Flpase recombinase and the subsequent recombination of Frt cassette, a fourth set of primers was used, designed to surround LoxP site (named Usp22 (2)) in order to detect the heterozygous mice with Usp22 cassette (figure 10a). Finally, Cre primers were used in order to select the mice that carried the tissue specific recombinase.

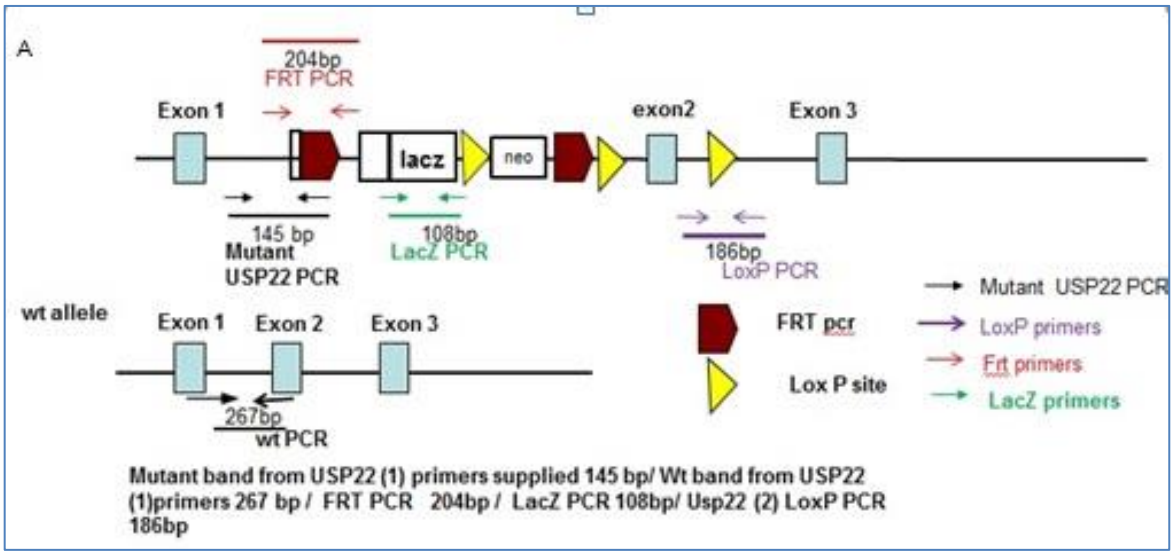

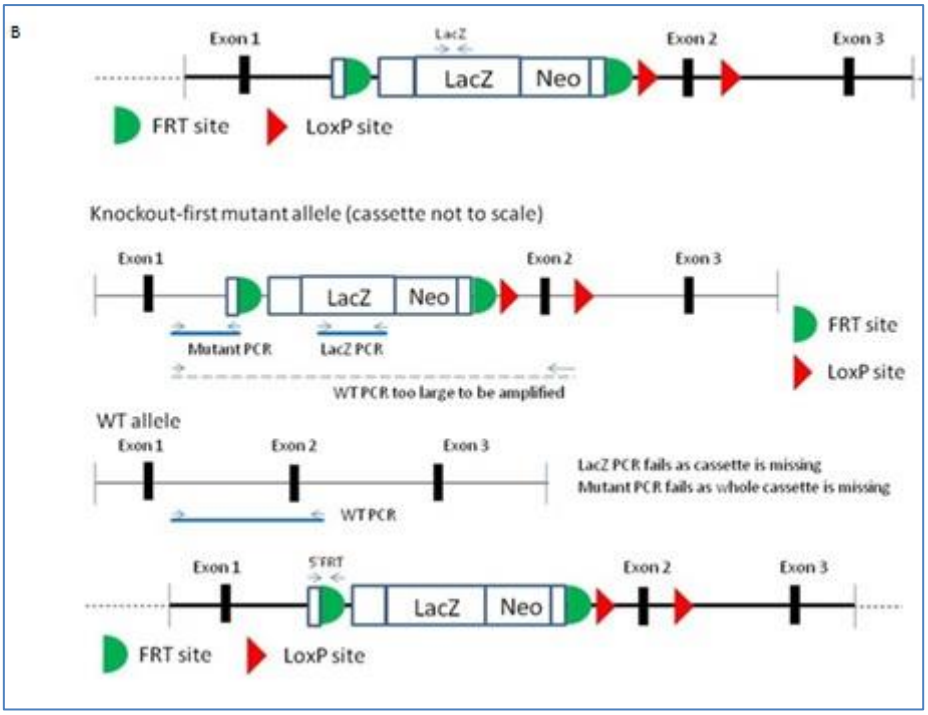

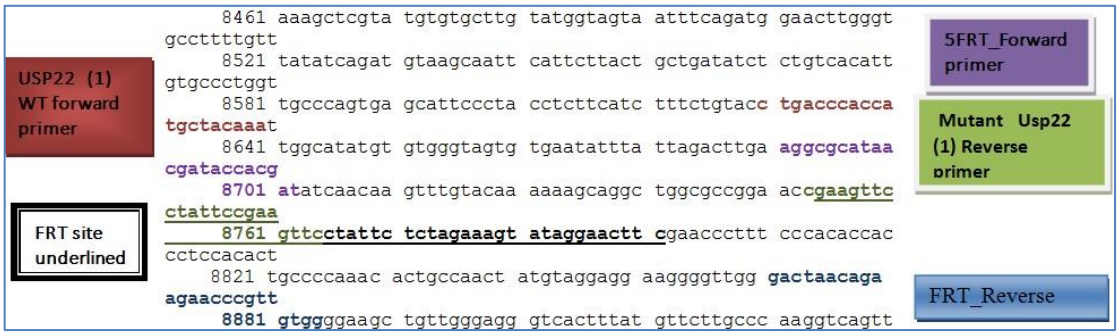

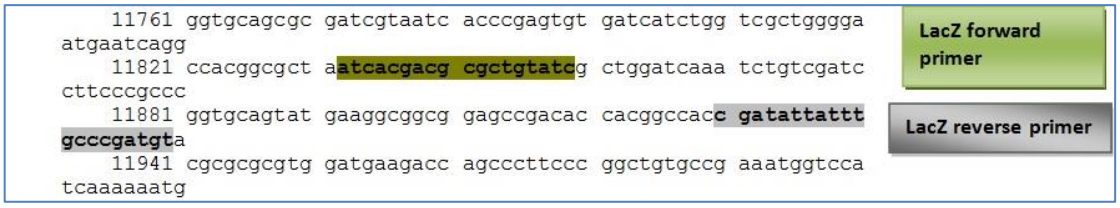

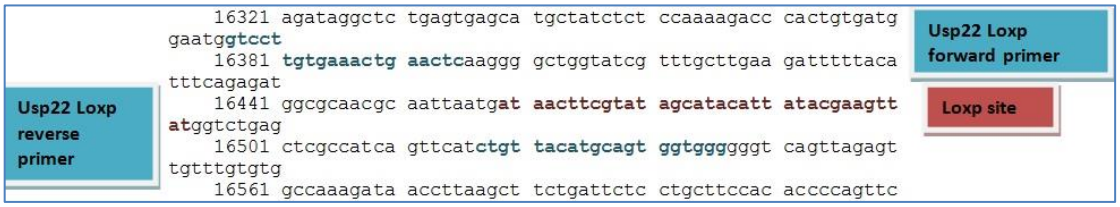

Figure 10: A) Overview of all the genotyping primers which are used for the genotyping of conditional knock-out mice with total scheme of primers at Usp22 cassette. B) More detailed scheme of Frt, LacZ, Usp22 (1) primers at Usp22 cassette

It must be noted that Flpase enzyme can function as Cre recombinase (figure 11a). For this reason, after Frt recombination, all potential heterozygous mice with Usp22 cassette destined for specific-knockout mice were cloned with specific set of primers in a distance of second Frt site in close proximity with fist Loxp site into p-GEMTeasy vector, followed by diagnostic digestions (Sal1-Nco1/ Nco1-Pst1/ DdeI) and direct sequencing (figure 11b; 12).

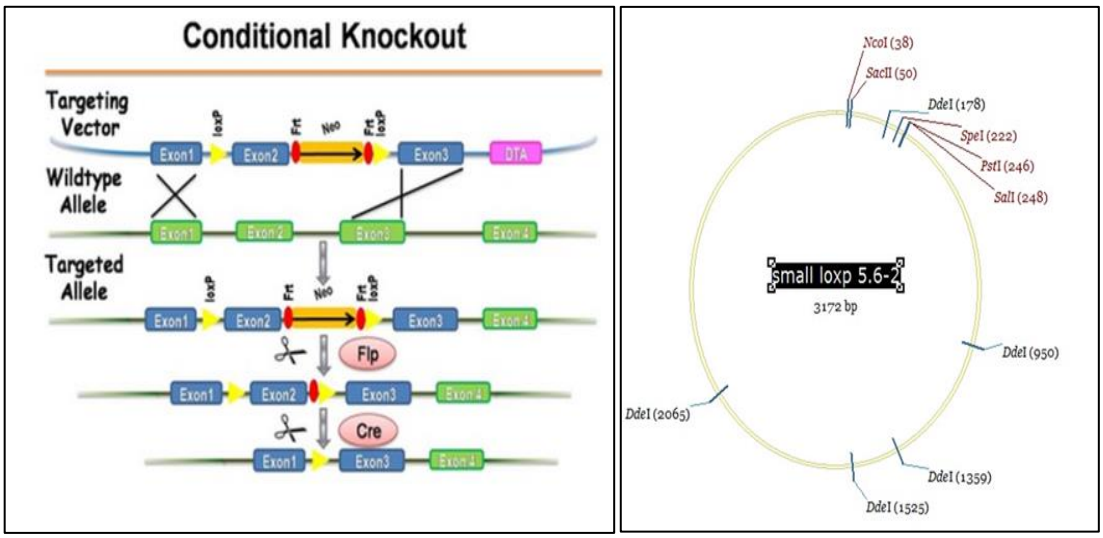

Figure 11: A) Scheme of generation of conditional knock-out mice B) Restriction map of heterozygous mice which were sent for direct sequencing for verification of loxP site C) Indicative results from sequencing.

FRT black underlined

15481 gcaattgttg ttgttaactt gtttattgca gcttataatg gttacaaata
aagcaatagc
15541 atcacaaatt tcacaaataa agcatttttt tcactgcatt ctagttgtgg
tttgtccaaa
15601 ctcatcaatg tatcttatca tgtctggatc cgggggtacc gcgtcga**gaa**
gttcctattc
15661 cgaagttcct attctctaga aagtatagga acttcgtcga g**ataacttcg**
tatagcatac
15721 attatacgaa gttatgtcga gatatctaga cccagctttc ttgtacaaag

Loxp site

Assay	5' Forward Name	5' Forward Sequence	3' Reverse Name	3' Reverse Sequence	Product size
Usp22	Usp22 (sequencing) F	GGA ACT TCG TCG AGA TAA CTT C	Usp22(sequencing) R	GCC TAC TGC GAC TAT AGA G	115nt

Figure 12: A distance of second Frt site in close proximity with fist Loxp site and a table of used primers for sequencing of Loxp sites. The sequence which is black underlined indicates the second Frt site and the sequence which is red in color, demonstrates the first Loxp site.

- **<u>Generation of Tg human Usp22 mice and Tg human mutant C185S mice</u>**

The preparation of the following constructs that will be used to microinject fertilized oocytes, has been initiated: The tagged cDNA of human Usp22 (pCMV-3HA-human USP22 was digested with Xhol1 and Not1) will be integrated into ERT vector, which contains the ligand binding domain of a mutant form of estrogen receptor and renders the expression of gene tamoxifen inducible. The pBluescript vector containinig the TTR1 will be cut with the StuI restriction enzyme and "filled in" with Klenow fragment of polymerase. The last step will be the blunt end ligation of the 3HA- h Usp22-ER1 tag in the pBluescript at the StuI enzyme (figure 13; 14).

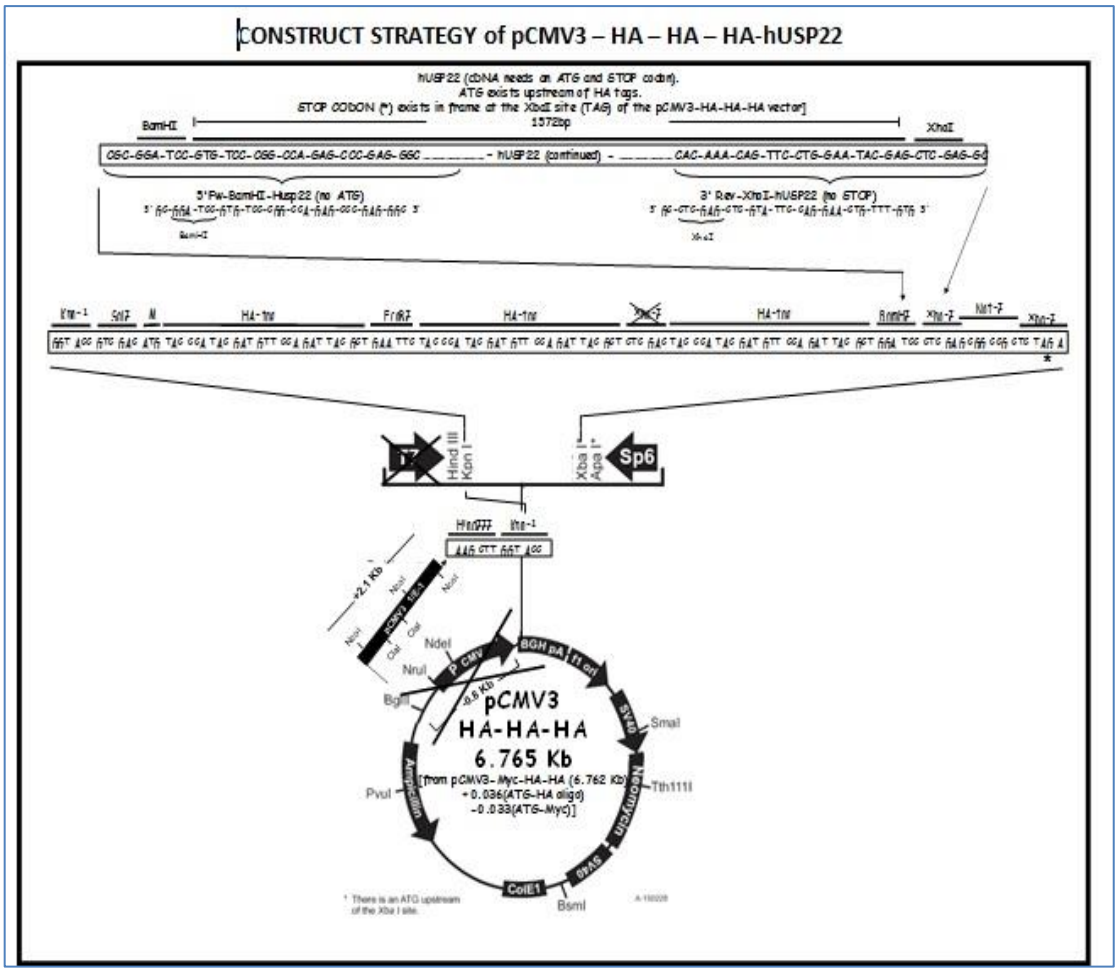

MAP of pCMV3 – HA – HA – HA-hUSP22

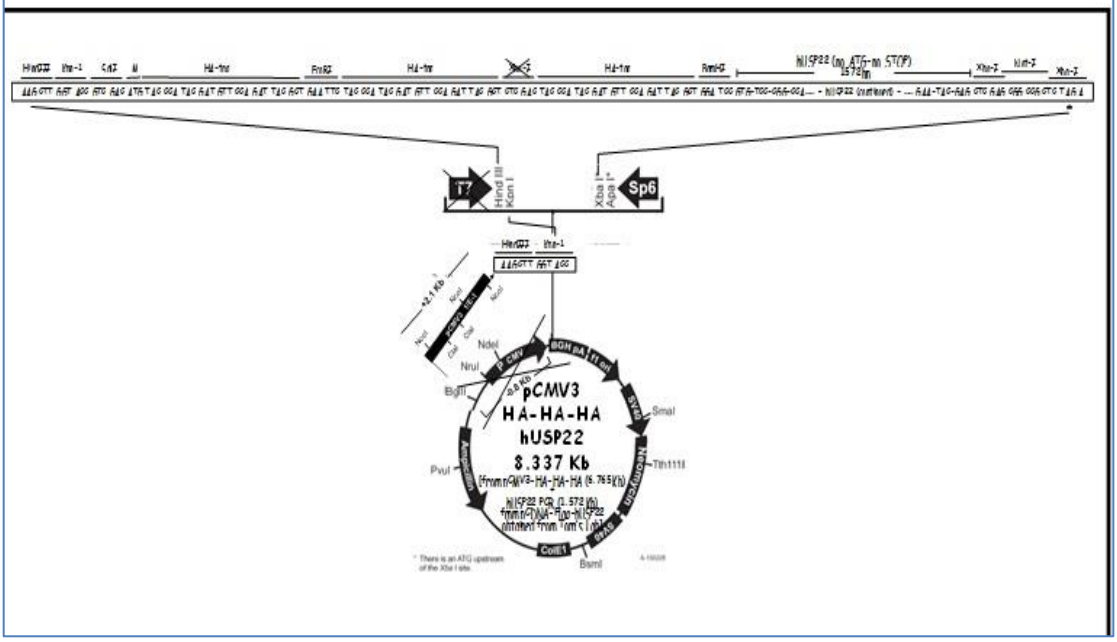

CONSTRUCT STRATEGY OF

pCMV3 – HA – HA – HA-hUSP22- (36/37)-h ER1(LBD) 847bp-1781bp (G400V/M543A/L544A)-IRES

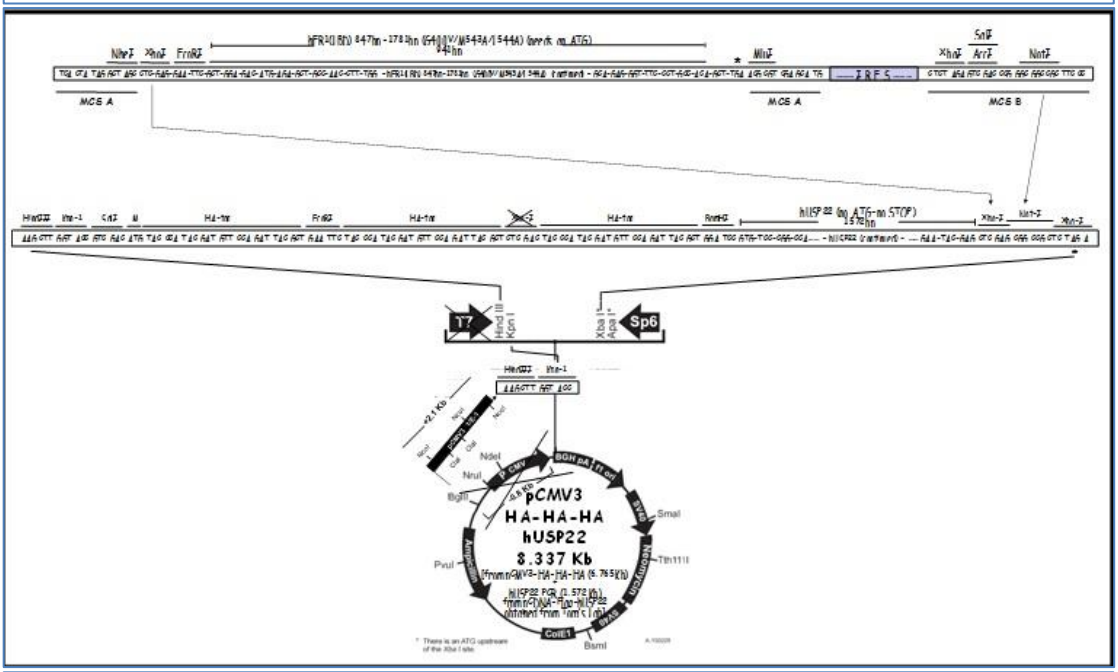

MAP OF

pCMV3 – HA – HA – HA-hUSP22- (36/37)-hER1(LBD) 847bp-1781bp (G400V/M543A/L544A)-IRES

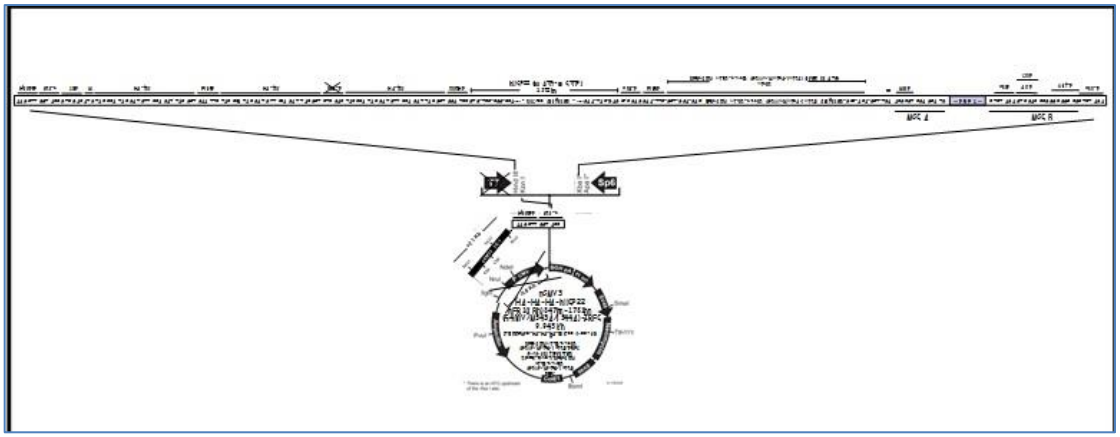

CONSTRUCT STRATEGY OF

p Bluescript-TTR1 – HA – HA – HA-hUSP22- h ER1(LBD) 847bp-1781bp (G400V/M543A/L544A)-IRES

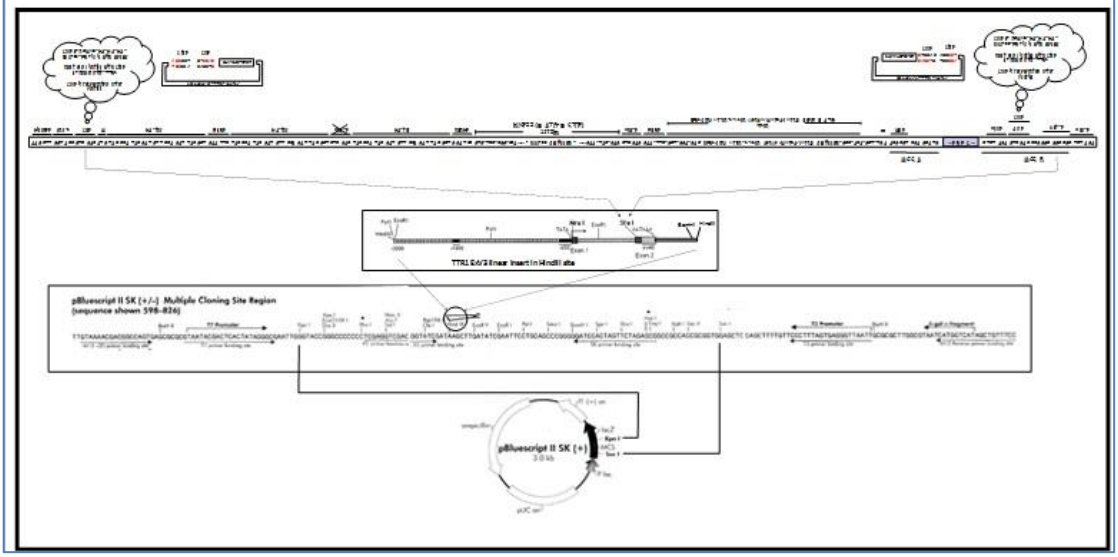

MAP OF

p Bluescript-TTR1 – HA – HA – HA-hUSP22- h ER1 (LBD) 847bp-1781bp (G400V/M543A/L544A)-IRES

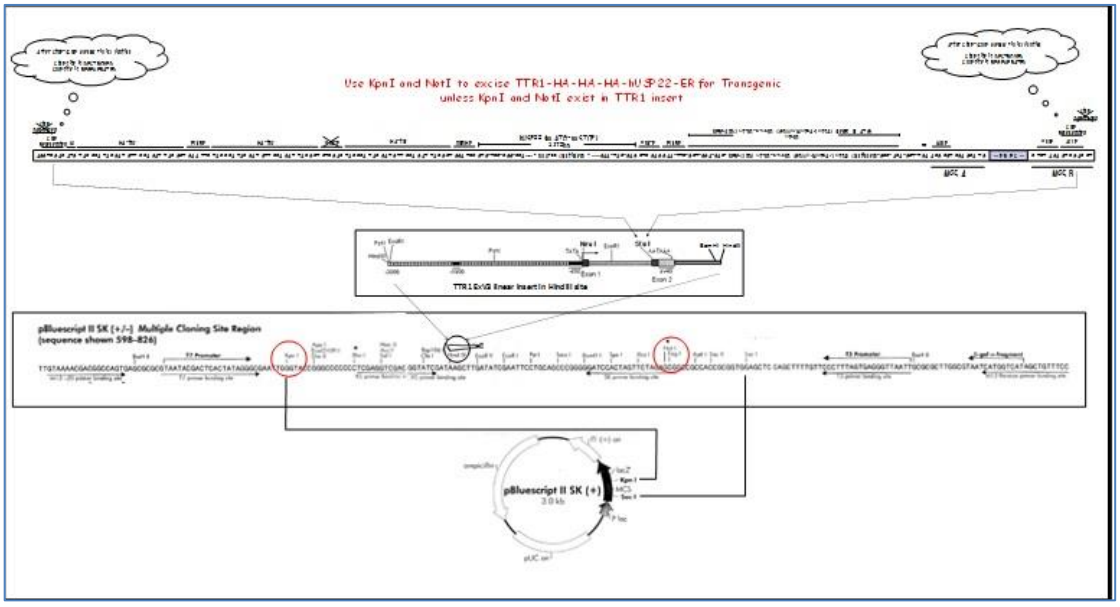

Figure 13: Cloning strategy and maps of Usp22-overexprsssing transgenic mice.

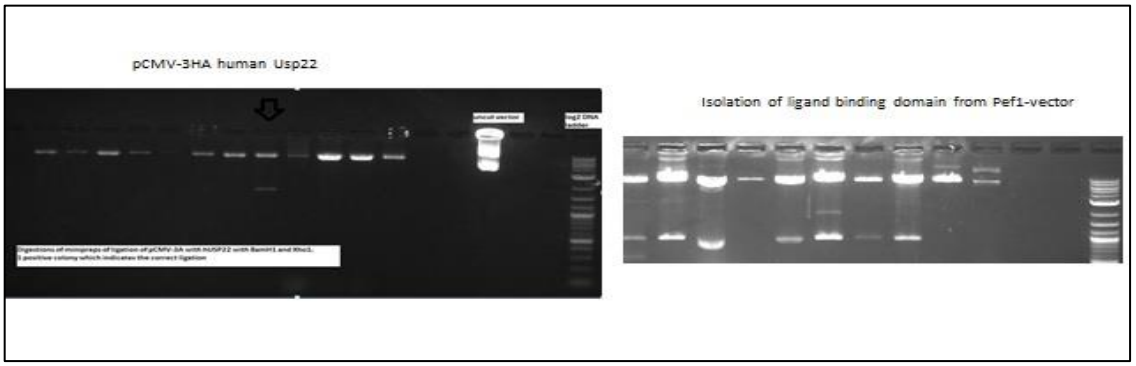

Figure 14: Agarose gel electrophoresis pictures showing the isolation of pCMV-3HA human Usp22 DNA and ligand binding domain DNA from Pef-1vector.

The generation of transgenic (Tg) mutant overexpressing human USP22 is performed with substitution of catalytic cysteine at residue 185 by serine (figure 15; Lin *et al.* 2012), its incorporation in 3HA-humanUSP22-ER1 tag and finally its blunt end ligation tag in the pBluescript at the StuI enzyme.

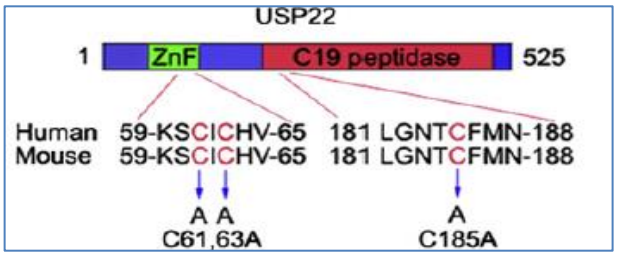

Figure 15: Schematic representation of USP22 and its point mutants. The conserved cysteine (C) residues either in the ZnF or the C19 peptidase domains were replaced by alanines (A) (Lin *et al.* 2012).

IV. Results Part B

Usp22 in cancer, liver regeneration, metabolic stress and liver development

Results-Part B

1. Usp22 overexpressed in cancerous liver

It was previously known that USP22 is overexpressed in several human types of cancer and so far all the knowledge comes from studies using cell lines. In order to monitor this *in vivo*, we examined the mRNA and protein levels of Usp22, in liver tumors isolated from mice that were subjected to DEN/TCPOBOP protocol (Gao. 2005; He and Karin. 2011).

In this protocol, the initial event caused by the chemical carcinogen DEN is death that induces an inflammatory response, creates a local environment that alters gene expression, stimulates cell proliferation and increases the population of mutant cells created by the initiator.

Initially, the Usp22 protein levels were evaluated in different cell lines. More specifically, cancerous HeLa cell line, T293 cells and T293 cells transfected with human Usp22 were used. Proteins were extracted from all of them in different ways (whole cell and nuclear extracts). Different commercial antibodies provided by the companies Abcam, Millipore, NBP1, Origene, Santa Cruz Biotechnology, Sigma and Thermo scientific were examined by western blot analysis (data not shown). Using T293 cells, transfected with human Usp22, it was confirmed that only the antibody (Ab) provided by Santa Cruz Biotechnology recognized the Usp22 protein (figure 16). However, the specificity of the antibodies will be confirmed when the Usp22-KO mice become available.

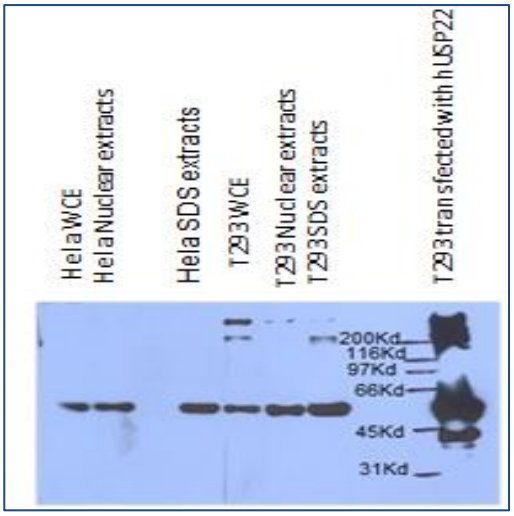

Figure 16: Western blot analysis of Usp22 (Santa Cruz Biotechnology) was performed in different cell lines (Hela, T293) and T293 cells transfected with human Usp22.

Thereafter, Usp22 protein levels were assessed in cancerous liver extracts compared to 8-month old male wild-type mice. As anticipated, increased Usp22 protein levels were observed in cancerous liver extracts when compared to the normal-non DEN/TCPOBOP treated liver controls (figure 17).

The relative mRNA levels of Usp22 were measured by qPCR and as indicated in the graph (figure 17 A), we observed a 9- fold induction of the cancerous samples over the controls.

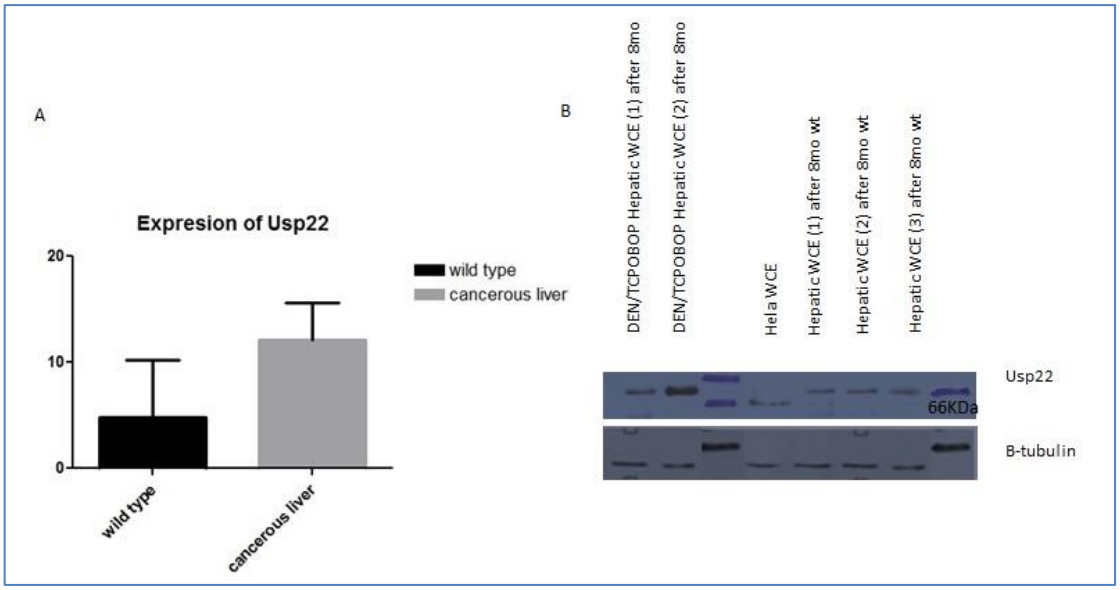

Figure 17: **The induction of Usp22 in chemical induced-model (DEN/TCPOBOP)**.A) The relative mRNA levels of Usp22 were normalized to GAPDH mRNA levels respectively. These data are presented as folds over values obtained from wild-type animals. These experiments were performed at least 3 times in 4 mice. B) Western blot analysis of whole cell extracts (WCE), nuclear extracts were blotted with Usp22 (Santa Cruz Biotechnology) and normalized with b-tubulin (Abcam).

2. Usp22 upregulated in proliferating hepatocytes

The liver appears to be unique among the other organs through its tremendous capacity to regenerate after injury. Even after resection of 2/3 of the liver through an experimental surgery which is called partial hepatectomy (PH), it can fully restore its mass in the normal levels.

Liver regeneration after partial hepatectomy indicates a growth response that culminates in hepatocyte replication and it is tightly controlled response to loss of liver mass, a complex chain of interrelated molecular and cellular events. This process has several important biological characteristics: (a) It is a process of compensatory hyperplasia rather than true regeneration in that removed parts do not grow back, instead the liver remnant increases in mass; (b) The process depends on the replication of all populations of cells within the liver, including hepatocytes, biliary epithelial cells and endothelial cells without the precipitation of stem cells (c) Replication of hepatocytes proceeds in a synchronous wave and is followed

(approximately 1 day later) by replication of non-parenchymal cells; (d) Growth terminates when liver mass reaches normal values (Diehl *et al.* 1996).

In order to investigate the role of Usp22 in normal cell cycle progression, 2-month old male wild-type mice were subjected to partial hepatectomy (PH). We selected to use 2-month old male wild-type mice in our experiments because the number of proliferating cells decreases with age, thus making regenerations slower and less complete in older animals. PH will be applied also to Usp22-deficient and human USP22 overexpressing animals of the same age, when those will be available. At different time points after PH, we performed Ki67 staining (figure 18) to estimate the proportion of cells that progresses through S phase of cell cycle.

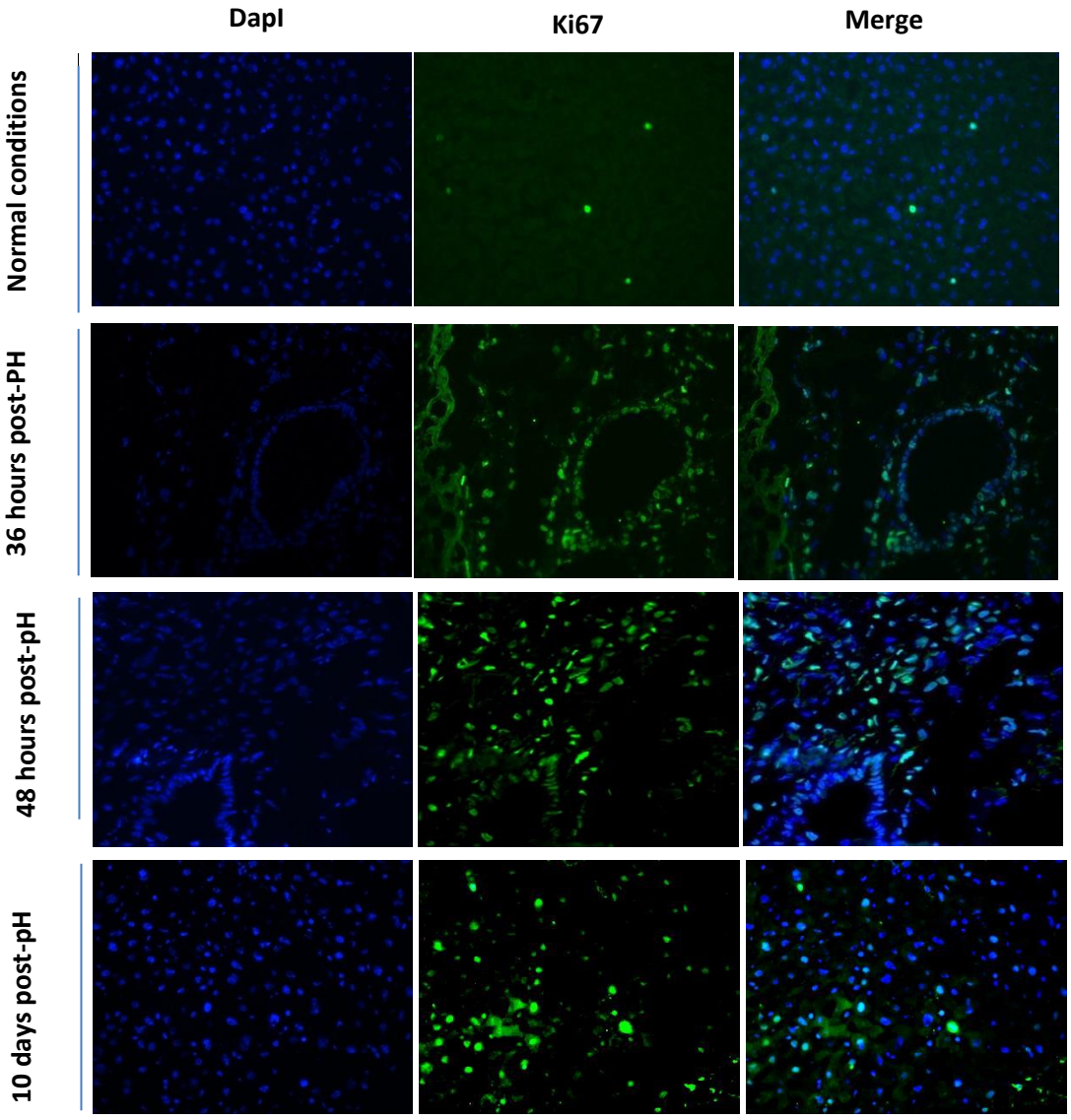

Figure 18: **Confirmation of liver sections at 2-month wild-type mice without partial hepatectomy with Ki67 staining. Immunohistological** staining of liver sections from liver cryosections after partial hepatectomy with Ki67 antibody. All the mice used at the experiments were 2 months old mice.

In parallel, Usp22 mRNA levels were evaluated at different time points: 36 hours after partial hepatectomy (when DNA synthesis begins), 48 hours (when DNA synthesis peaks) and 10 days (when liver regeneration has been completed). Differences in the expression levels were observed within the three groups after liver resection compared to control group. Usp22 was upregulated at all the time points tested. More specifically, the mRNA expression of Usp22 started to increase 36 hours after partial hepatectomy. It continued increasing within 48 hours and culminated within 10 days when liver had been fully regenerated. Results from quantitive Real-time PCR were obtained using 6 mice at each time point, so that statistical significance with t-test could be attained (figure 19).

At the protein level, as indicated by Western Blot analysis (Figure 20), Usp22 showed a similar but not identical trend. More specifically, Usp22 protein levels increased within 36 hours post-PH, reached a peak at 48 hours post- PH and were restored to normal levels on the 10^{th} day after liver resection, when compared to the littermate control mice. Using the Image J program we could calculate the folds of induction at each timepoint. On average, within 36 hours post-PH, Usp22 protein levels were 2. 5-folds more and in 48 hours were 8.48-folds more compared to the littermate controls (figure 20). Finally, within 10 days post-PH no significant difference was observed contrary to the qPCR results. Consequently, these results indicate that Usp22 may be useful as a marker for the entry of hepatocytes at S phase of the cell cycle (G1/S transition).

The variance between the results obtained by qPCR and Western Blot analysis within 10 days post-PH timepoint could be explained, if Usp22 levels are not only regulated transcriptionally but also post-translationally. In this case, the potential post-translational modification at Usp22 would affect the protein stability. This, however, requires further investigation.

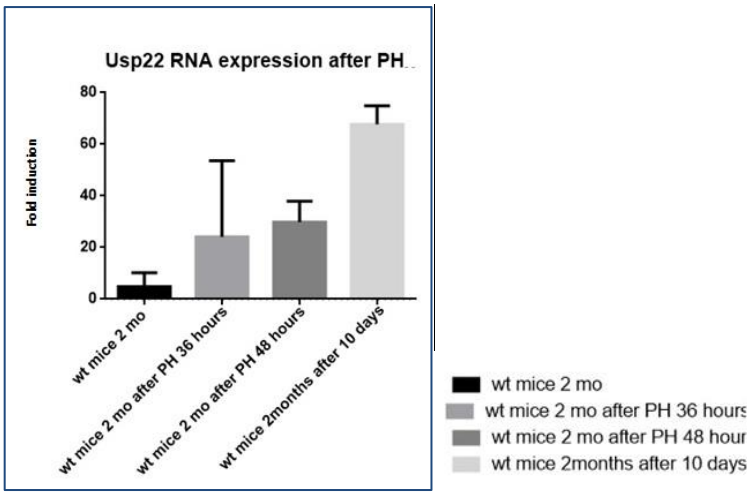

Figure 19: **Transcriptional up regulation of Usp22 within 36 h, 48 h and 10 days after Partial Hepatectomy** Usp22 mRNA levels of wild-type mice after partial hepatectomy within 36/48 hours, 10 days were normalized to GAPDH mRNA levels. These data are presented as fold over values obtained from wild-type animals. These experiments were performed at 6 mice (experiment repeated 3 times).

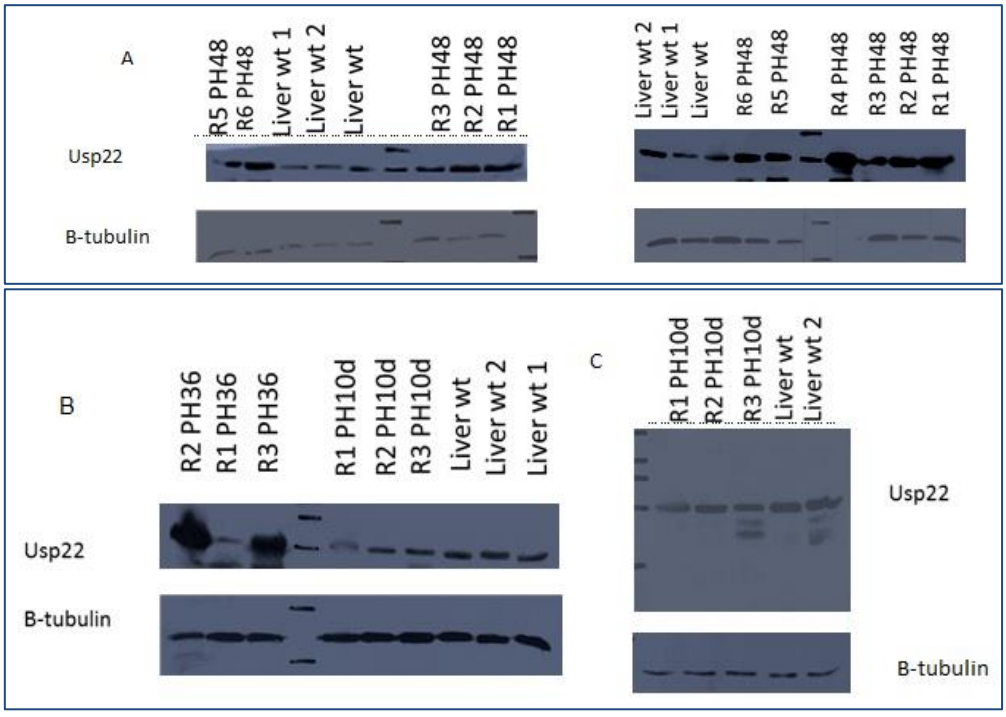

Figure 20: **The Cycling of Usp22 during Liver Regeneration** A) Western blot analysis of liver extracts was blotted with Usp22 and normalized with b-tubulin in wild-type mice after partial hepatectomy within 48 hours compared to littermate controls. B). Western blot analysis of liver extracts was blotted with Usp22 and normalized with b-tubulin (Abcam) in wild-type mice after partial hepatectomy within 36hours, 10 days compared to littermate controls. The enrichments at partial hepatectomy liver extracts within 36 hours, 48 hours were processed with Image J programme and calculated using t-test. The experiments were performed at least 3 times in 6 mice (selected 3 mice in figure and repeated 6 times). All the mice were 2-month old male wild-type mice.

It is noteworthy, that the enrichment of Usp22 in the regenerative "proliferating" liver was much higher than in cancerous livers (figure 21). Given that its significance in cancer has been already verified and that cancer is strongly associated with changes in the cell cycle machinery, it would be very interesting to investigate its role in cell proliferation.

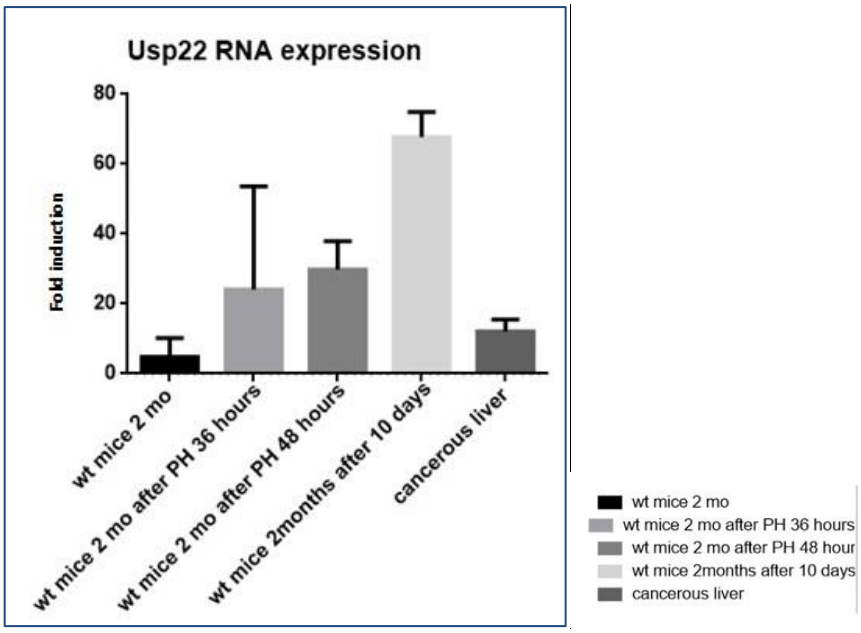

Figure 21: **Relative mRNA levels of Usp22 in cancerous and regenerative livers compared to littermate controls.** The Usp22 mRNA levels at wild-type mice after partial hepatectomy within 36 / 48 hours and 10 days were normalized to GAPDH mRNA levels. These data are presented as fold over values obtained from wild-type animals. These experiments were performed at least 3 times in 6 mice. The enrichment of Usp22 in liver regenerative liver is higher than cancerous livers or not-treated wild-type mice that had the lowest levels. All the mice used at experiments were male and 2 months years old.

3. Intracellular localization of Usp22 does not change in cancerous and regenerative liver

Previous studies have indicated that Usp22 function may be regulated by nucleocytoplasmic shuttling (Atanassov *et al.* 2009; Atanassov *et al.* 2011; Rodriquez-Navarro. 2009; Xiong *et al.* 2014; Zhang *et al.* 2008).

To investigate this scenario, we performed immunohistochemistry assays in liver under conditions of induced hepatocarcinogenesis and liver regeneration as well as in normal littermate controls. Usp22 was mainly nuclear, although some cytoplasmic staining could be

observed in untreated control samples. Nuclear accumulation was slightly more pronounced in cancerous and regenerative liver (figure 22, 23). Intact liver sections stained with HNF4 (hepatocyte marker), were used as positive control for the experimental procedure (figure 24).

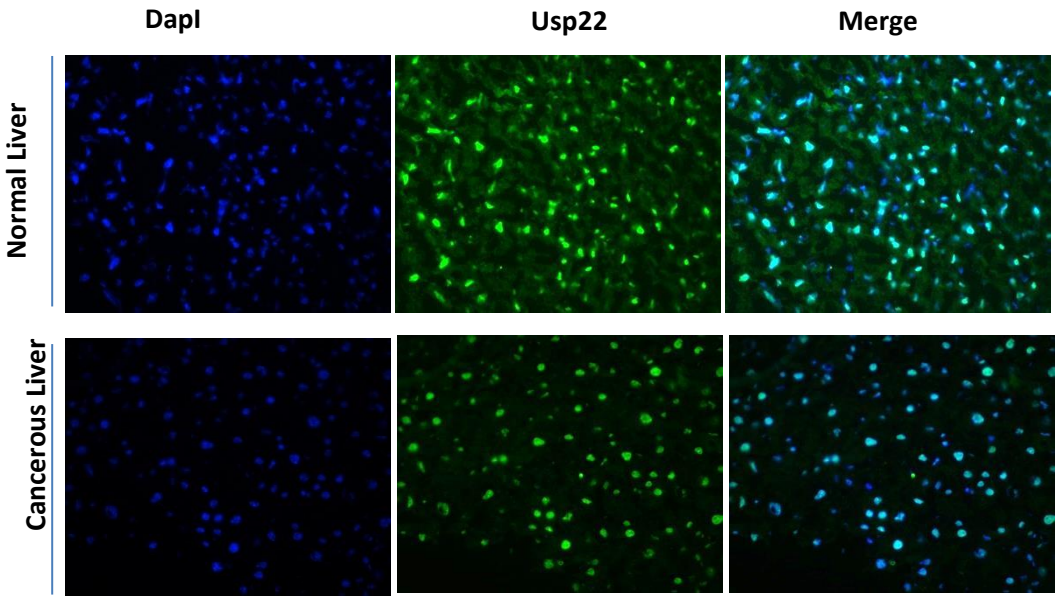

Figure 22: **Nuclear accumulation of Usp22 in cancerous liver** .Immunohistological staining of liver cryosections from non-treated and DEN treated wild-type mice with Usp22 antibody (left: DapI, middle: Usp22, right: merge). All the mice were 2-month old male wild-type mice.

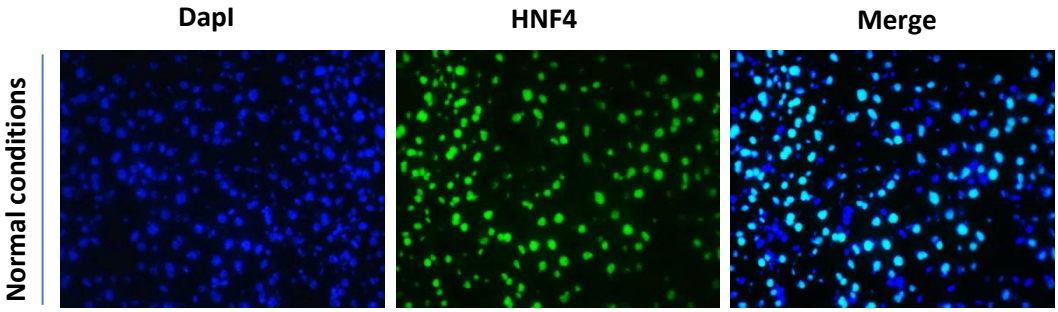

Figure 23**: HNF4 control.** Immunohistological staining of liver sections from liver cryosections of wild type mice with HNF4 antibody (left: DapI, middle: HNF4, right: merge). All the mice were 2-month old male wild-type mice.

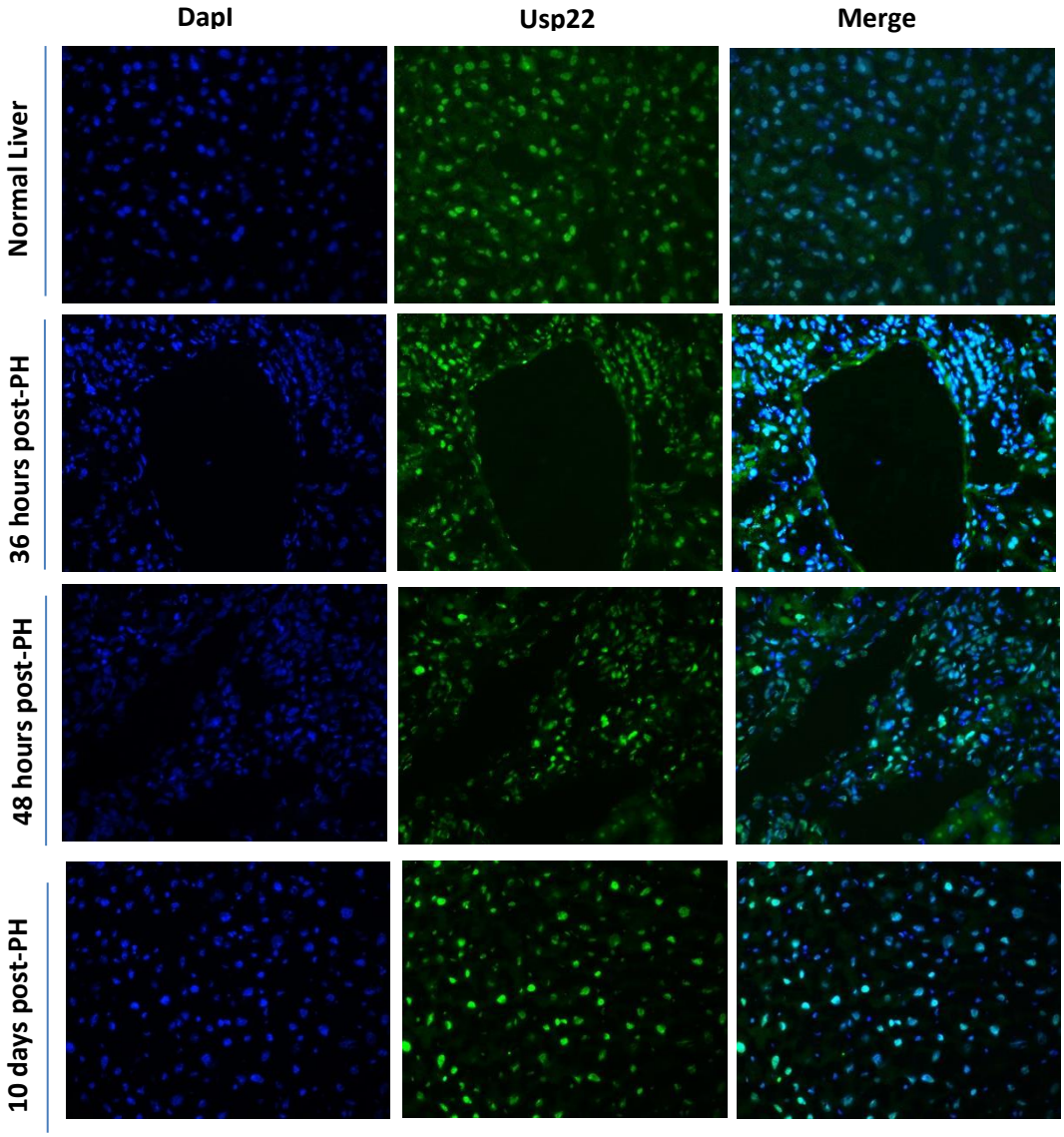

Figure 24: **Nuclear localization of Usp22 upon 36, 48 hours and 10 days partial hepatectomy.** Immunohistological staining of liver sections from liver cryosections after partial hepatectomy within 36, 48 hours and 10 days with Usp22 antibody. This staining was also performed at normal liver (left: DapI, middle: Usp22, right: merge). All the mice were 2-month old male wild-type mice.

4. Nuclear accumulation of GCN5 in cancerous liver

USP22 was identified as a bona fide component of the human SAGA general transcription factor complex (Krebs *et al.* 2011) suggesting that targeted deubiquitination of histones is intrinsically linked to transcription activation and epigenetic regulation (Pijnappel *et al.* 2008). The simultaneous partitioning of histone acetyltransferase (GCN5) and histone deubiquitinase (USP22) enzymatic activities within the same general transcription factor complex proposes that a potential crosstalk between acetylation and ubiquitination may play a role in gene activation. Moreover, GCN5 and USP22 as well as other SAGA subunits, are cooperating and acting as cofactors for the full transcriptional activity by nuclear receptors (Wallberg *et al.*2000; Yanagisawa *et al.* 2002; Zhao *et al.* 2008).

Initially, Gcn5 was detected by Western Blot in cancerous Hela and T293 cell line as a band of 110 kDa (figure 25). No band was detected at the Wi38 (human fibroblasts) extracts – either nuclear or whole cell extracts- which could be partially explained by a quantity dependent limitation in the efficiency of the antibody used, as well as by the fact that GCN5 is overexpressed in cancerous samples.

By immunocytochemistry analysis it was observed that Gcn5 was accumulated in the nucleus in cancerous liver samples (figure 26), whereas, it was detected both in the cytoplasmic and nuclear compartment in untreated littermate controls (figure 26). The same nuclear accumulation in cancerous liver samples was also observed in the case of Usp22 (figure 22). For instance, the mainly cytoplasmic deposition of Gcn5 in the untreated controls seems to be a paradox (since it is more likely to have nuclear localization because of its HAT activity). However, it is known that Gcn5 can extend its function in the cytoplasm in nascent histone and non-histone substrates (Jin *et al.* 2014). Thus, the observed Gcn5 translocation and nuclear accumulation might be of particular interest especially when Usp22 follows the same scheme. Further experiments and optimization of experimental conditions are required in order to provide insights into this issue.

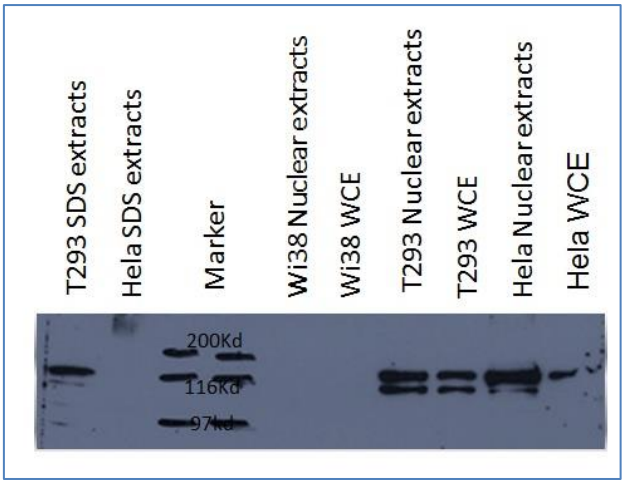

Figure 25: Western blot analysis of Gcn5 at different cell lines (Hela, T293 and Wi-38). Different extracts (whole cell extracts (WCE), nuclear extracts, SDS extracts) were blotted with primary antibody against Gcn5 (Santa Cruz Biotechnology).

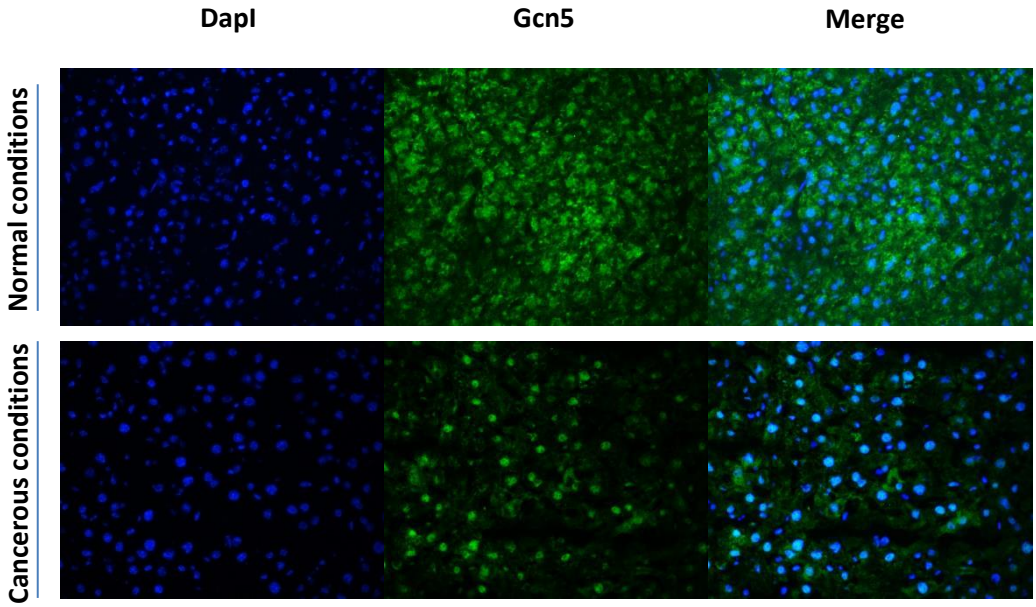

Figure 26: **Nuclear accumulation of Gcn5 upon cancerous stimulus**. Immunohistological staining of liver sections from cancerous cryosections 5µm of induced model of hepatocarcinogenesis with Gcn5 antibody (left: DapI, middle: Gcn5, right: merge). All the mice were 2-month old male wild-type mice.

5. Metabolic stress leads to upregulation of Usp22 in liver

To investigate the role of Usp22 in fasting response, initially we estimated its mRNA and protein levels in the livers of 24-hour fasted mice. At the mRNA level, Usp22 showed a more than 100 folds of induction in the fasting livers (figure 27 A). Western blot (Figure 27 B) analysis revealed an upregulation of Usp22 after 24h fasting compared to the littermate controls. Further studies are still needed, nevertheless, to dissect the role of Usp22 in fasting-induced metabolic control mechanisms.

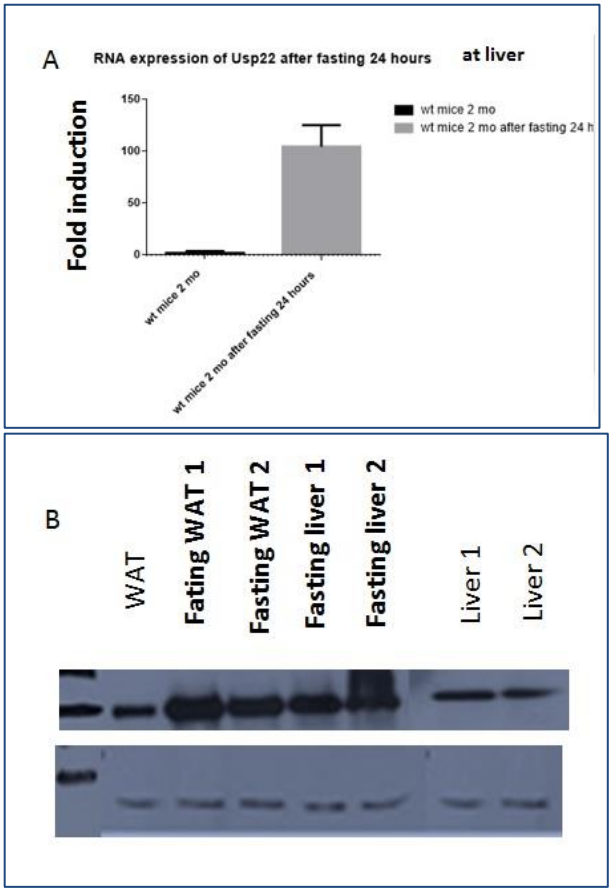

Figure 27: **The induction of Usp22 after fasting 24 hours at wild-type mice**).A) mRNA levels of Usp22 were normalized to GAPDH mRNA. These data are presented as fold over values obtained from wild-type animals. These experiments were performed at least 3 times in 4 mice B) Western blot analysis of liver extracts (whole cell extracts (WCE), white adipose tissue extracts (WCE) extracts was blotted with Usp22 (Santa Cruz Biotechnology) and normalized with b-tubulin (Abcam).

6. Usp22 mRNA levels are relatively high and do not change during development

The mRNA levels of Usp22 during liver development from RNA-sequencing data were monitored in our lab (figure 28). Results from RNA sequencing indicated that Usp22 mRNA did not fluctuate significantly during liver development.

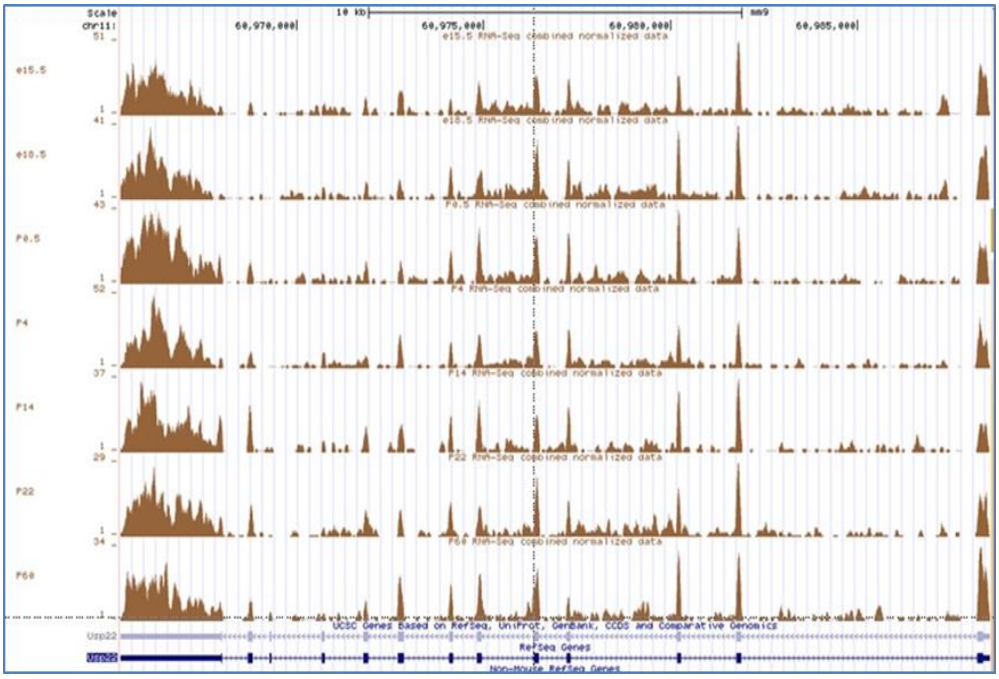

Figure 28: Distribution of expression levels of Usp22 according to RNA seq data which were available in the lab.

V. Discussion and future plans

The present work provides some preliminary data of the work planned towards understanding the impact of Usp22 in hepatocarcinogenesis, liver regeneration and metabolism. Our experiments so far indicate aberrant expression in cancerous, regenerative and fasting liver extracts compared to littermate controls, which can be attributed to both intrinsic and extrinsic factors. Overexpression of Usp22 was observed in mice with DEN-induced hepatocarcinoma, in regenerating livers after partial hepatectomy and in livers of fasted mice.

These preliminary data provide the starting point for more detailed investigations on Usp22 and its targets. Instrumental to these future studies will be the new animal models we developed. These models include liver-specific Usp22 KO mice and transgenic mice overexpressing human USP22 in the liver. Once these models are available, we will be able to assess directly the role of Usp22 in cell proliferation, HCC development and fasting response. The experimental models will be subjected to extensive phenotypic and histological analysis before further studies. Routine assays will involve recording animal growth and organ sizes, hematoxylin eosin staining of sections from adult organs and whole mount sections of embryos, RT-PCR, immunostaining and western blot assays for targeted and transgene expression, as well as immunostaining with lineage and cell type-specific markers. These studies will provide initial insights into the phenotypes induced by loss of USP22.

Extensive histopathological analysis will include stainings for proliferation markers (BrdU, Ki67, CyclinD1), for oncofetal hepatic markers (Afp, EPCAM, A6), stem cell markers (CTGF, Glypican, CD133) and markers associated with stem cell pluripotency (Nanog, Sox2 and Klf4). The expression of the latter set of markers has recently been identified in our lab as characteristic to highly aggressive hepatocellular carcinoma.

We will also measure potential global changes in histone modifications (H2A, H2B ubiquitination, H3K4 methylations) by western blot analysis and immunohistochemistry.

Specifically, gene specific alterations in histone modification patterns will be monitored by ChIP-seq. This will be supplemented by Chip-seq for Usp22 and by global gene expression profiling using RNA-seq in the adult livers of Usp22 KO and overexpressing transgenic mice.

Acknowledgements

First of all, I would like to thank Dr. Talianidis I, for the guidance to complete my thesis. His comments were always thoughtful and significant.

I would also like to express my thanks to the staff of our lab for their invaluable help: Antonoglou A., Haroniti A., Gargani S., Karagianni Y., Moulos P., Nikolaou K., Papageorgopoulou E., Rubio T., Sarris M. and Saviolaki D.

My thanks to the researcher Hatzis P. who was extremely helpful whenever I needed his help. Giakountis A., Haronoti A., Karagianni Y. and Saviolaki D. were also willing to help me solve all the problems concerning technical matters. Their help and comments proved to be invaluable.

I owe particular thanks to the vet, Ntafis V. for his support and constant help in how to handle mice and perform partial hepatectomy on them. I also express my thanks to Kontaki X. who offered me her help whenever I asked her for it.

My cordial thanks to the director of the post-graduate programme, Kardassis D and Savvakis C. for their support and their continuous encouragement during my post-graduate study.

Last but not least, I am grateful to my parents and my brother for their continuous encouragement.

References

Ao N., Liu Y., Feng H., Bian X., Li Z., Gu B., Zhao X. and Liu Y. 2014. Ubiquitin-specific peptidase Usp22 negatively regulates the STAT signaling pathway by deubiquitinating SIRT1. Cellular Physiology and Biochemistry 33: 1863-1875.

Armour S.M., Bennett E.J., Braun C.R., Zhang X., Mc.Mahon S.B., Gygi S.P., Harper J.W. and Sinclair D.A. 2013. A high-confidence interaction map identifies SIRT1 as a mediator of acetylation of Usp22 and the Saga coactivator complex. Molecular and Cellular Biology 33 (8): 1487-1502.

Atanassov B.S. and Dent S.Y.R. 2011. Usp22 regulates cell proliferation by deubiquitinating the transcriptional regulator FBP1. EMBO Reports 9 (12): 924-930.

Atanassov B.S., Evrard Y.A., Multani A.S., Zhang Z., Tora L., Devys D., Chang S. and Dent S.Y.R. 2009. Gcn5 and Saga regulate shelterin protein turnover and telomere maintenance. Molecular Cell 35: 352-364.

Atanassov B.S., Koutelou E. and Dent S.Y. 2011. The role of deubiquitinating enzymes in chromatin regulation. FEBS letter 585 (13): 2016-2023.

Bai P., Cantó C., Oudart H., Brunyánszki A., Cen Y., Thomas C., Yamamoto H., Huber A., Kiss B., Houtkooper R.H. 2011. PARP-1 inhibition increases mitochondrial metabolism through SIRT1 activation. Cell Metabolism 13: 461–468.

Baker S.P. and Grant P.A. 2007. The SAGA continues: expanding a cellular role of a transcriptional co-activator complex. Oncogene 26 (37): 5329-5340.

Balasubramanian R., Pray-Grant M.G., Selleck W., Grant P.A., Tan S. 2002. Role of the Ada2 and Ada3 transcriptional coactivators in histone acetylation. J Biol Chem 277: 7989-7995.
Barbaric S., Reinke H. and Horz, W. 2003. Molecular and Cellular . Biology 23: 3468-3476.

Berezovska O.P., Glinskii A.B., Yang Z., Li X.M., Hoffman R.M., Glinsky G.V. 2006. Essential role for activation of the Polycomb group (PcG) protein chromatin silencing pathway in metastatic prostate cancer. Cell Cycle 5(16): 1886–1901

Bhaumik S.R., Raha T., Aiello D.P., Green M.R. 2004. In vivo target of a transcriptional activator revealed by fluorescence resonance energy transfer. Genes and Development 18: 333-343.

Bonnet J., Wang C., Baptista T., Vincent S.D., Hsiao W., Stierle M., Kao C., Tora L. and Devys D. 2014. The SAGA coactivator complex acts on the whole transcribed genome and is required for RNA polymerase II transcription. Genes and Development 28: 1999-2012.

Brooks C.L. and Gu W. 2009. How does Sirt1 affect metabolism, senescence and cancer. Nature Reviews Cancer 9 (2): 123-129.

Cantó C., Houtkooper R.H., Pirinen E., Youn D.Y., Oosterveer M.H., Cen Y., Fernandez-Marcos P.J., Yamamoto H., Andreux P.A., Cettour-Rose P. 2012. The NAD (+) precursor nicotinamide riboside enhances oxidative metabolism and protects against high-fat diet-induced obesity. Cell Metabolism 15: 838–847

Cerutti R., Pirinen E., Lamperti C., Marchet S., Sauve A.A., Li W., Leoni V., Schon E., Dantzer F., Auwerx J., Viscomi C. and Zeviani M. 2014. NAD^+ -dependent activation of Sirt1 corrects the phenotype in a mouse model of mitochondrial disease. Cell metabolism 19: 1042-1049.

Chen D., Bruno J., Easlon E., Lin S.J., Cheng H.L., Alt F.W. et al. 2008. Tissue-specific regulation of SIRT1 by calorie restriction. Genes and Development. 22(13): 1753–7.

Chipumuro E. and Henriksen M.A. 2012. The ubiquitin hydrolase USP22 contributes to 3'-end processing of JAK-STAT-inducible genes. FASEB journal 26: 842-54

Clague M.J., Barsukov I., Coulson J.M., Liu H., Rigden D.J. & Urbe S. 2012. Deubiquitylases from genes to organism. Annual Review of Physiology 93: 1289-1315.

Clements A., Poux A.N., Lo W.S., Pillus L., Berger S.L. and Marmonstein R. 2003. Structural basis for histone and phosphohistone binding by the GCN5 histone acetylatransferase. Mol. Cell 12: 461-473.

Cole A.J., Clifton-Bligh R. and Marsh D.J. 2014. Histone H2B monoubiquitination-roles to play in human malignancy. Endocrin Related Cancer.

Colland F. 2010. The therapeutic potential of deubiquitinating enzyme inhibitors. Biochem Society Transactions 38: 137-143.

Dai W., Yao Y., Zhou Q. and Sun C. 2014. Ubiquitin-specific peptidase 22, a histone deubiquitinating enzyme, is a novel poor prognostic factor for salivary adenoid cystic carcinoma. Plos One 9 (1):e87148.

Daniel J.A., Torok M.S., Sun Z., Schieltz D., Allis D., Yates III. J.R. and Grant P.A. 2004. Genes: Structure and regulation: Deubiquitination of histone H2B by a yeast acetylatransferase complex regulates transcription. The Journal of Biological Chemistry 279:1867-1871.

Dawson M.A., Kouzarides T. & Huntly B.J. 2012. Targeting epigenetic readers in cancer. The New England Journal of Medicine 367: 647-657.

Dubik D., Dembinski T.C., Shiu R.P. 1987. Stimulation of c-myc oncogene expression associated with estrogen-induced proliferation of human breast cancer cells. Cancer Research 47: 6517-21.

Faller S., Strosing K.M., Ryter S.W., Buerkle H., Loop T., Schmidt R. and Hoetzel A. 2012.The volatile anesthetic isoflurane prevents ventilator-induced lung injury via phosphoinositode 3-kinase/Akt signaling in mice. Anesthesia and Analgesia 114 (4): 747-756.

Flaus A. and Owen-Hughes T. 2004. Mechanisms for ATP-dependent chromatin remodeling: Farewell to the tuna-canoctamer? Current Opinion in Genetics and Development 14: 165-173.

Feige J.N., Auwerx J. 2007. DisSIRTing on LXR and cholesterol metabolism. Cell Metabolism (5): 343–5.

Grant P.A., Duggan L., Cote J., Roberts S.M., Brownell J.E., Candau R., Ohba R., Owen-Hughes T., Allis C.D., Winston F. et al.1997. Yeast Gcn5 functions in two multisubunit complexes to acetylate nucleosomal histones: Characterization of an Ada complex and the SAGA (Spt/Ada) complex. Genes and Development. 11: 1640-1650.

Gao B.2005. Cytokines, STATs and liver disease. Cellular and Molecular Immunology 2: 92–100.

Gehart-Hines Z., Dominy J.E., Blatter S.M., Jedrychowski M.P., Banks A.S., Lim J., Chim H., Gygi S.P. and Puigserver.2011. The cAMP/PPKA pathway rapidly activates Sirt1 to promote fatty acid oxidation independently of changes in NAD^+. Molecular Cell. 44: 851-863.

Glinsky G.V., Berezovska O. & Glinskii A.B. 2005 Microarray analysis identifies a death-from cancer signature predicting therapy failure in patients with multiple types of cancer. The Journal of Clinical Investigation 115: 1503-1521.

Glinsky G.V. 2006. Genomic modules of metastatic cancer: functional analysis of death-from-cancer signature genes reveals aneuploid, anoikis-resistant, metastasis-enabling phenotype with altered cell cycle control and activated Polycomb Group (PcG) protein chromatin silencing pathway. Cell Cycle 5: 1208–16.

Goldknopf, I.L., Taylor C.W., Baum R.M., Yeoman L.C., Olson M.O., Prestayko A.W. and Busch H. 1975. Isolation and characterization of protein A24, a "histone-like" nonhistone chromosomal protein. The Journal of Biological Chemistry250: 7182–7187.

Grant P.A., Schieltz D., Pray-Grant M.G., Yates J.R. 3rd, Workman J.L. 1998. The ATM-related cofactor Tra1 is a component of the purified SAGA complex. Molecular Cell 2: 863-867.

Greenblatt J.F. and Berger S.L. 2005. H2B ubiquitin protease Ubp8 and Sgf11 constitute a discrete functional module within the Saccharomyces cerevisiae SAGA complex. Molecular and Cellular Biology25: 1162-1172.

Guarente L. 2006. Sirtuins as potential targets for metabolic syndrome. Nature 444 (7121): 868–74.

Gurel B., Iwata T., Koh C.M., Jenkins R.B., Lan F., Van Dang C. et al. 2008. Nuclear MYC protein overexpression is an early alteration in human prostate carcinogenesis. Modern pathology: an official journal of the United States and Canadian Academy of Pathology, Inc.; 21: 1156-67.

Haglund K. and Dikic I. 2005. Ubiquitylation and cell signaling. EMBO Journal 24: 3353-3359.

Hagopian K., Ramsey J.J., Weindruch R. 2003. Influence of age and caloric restriction on liver glycolytic enzyme activities and metabolite concentrations in mice. Experimental Gerontology 38(3): 253–266.

He G. and Karin M. 2011. NF-kB and STAT3-key players in liver inflammation and cancer, Cell Research 21: 159-168.

Henikoff S. 2005. Histone modifications. Combinatorial complexity or cumulative simplicity? Proceedings of the National Academy of Sciences of the United States of America.102: 5308-5309.

Henry K.W., Wyce A., Lo W.S., Duggan L.J., Emre N.C., Kao C.F., Pillus L., Shilatifard A., Osley M.A. and Berger S.L. 2003. Transcriptional activation via sequential histone H2B ubiquitylation and deubiquitylation, mediated by SAGA-associated Ubp8. Genes and Development 17: 2648-2663.

Huang H., Sabari B.R., Garcia B.A., Allis C.D. and Zhao Y. 2014. Snapshot: Histone modifications. Cell 159. DOI http://dx.doi.org/10.1016/j.cell.2014.09.037.

Huisinga K. L. and Pugh B. F. 2004. A genome-wide housekeeping role for TFIID and a highly regulated stress-related role for SAGA in Saccharomyces cerevisiae. Mol. Cell 13: 573-585.

Hwang, W.W., Venkatasubrahmanyam, S., Ianculescu, A.G., Tong, A., Boone, C., and Madhani, H.D. 2003. A conserved RING finger protein required for histone H2B monoubiquitination and cell size control. Molecular Cell 11: 261–266

Ingvarsdottir K., Krogan N.J., Emre N.C., Wyce A., Thompson N.J., Emili A., Hughes T.R., Greenblatt J.F. and Berger S.L. 2005. H2B ubiquitin protease Ubp8 and Sgf11 constitute a discrete functional module within the Saccharomyces cerevisiae SAGA complex. Molecular and Cellular Biology 25: 1162-1172.

Jacq X., Kemp M., Martin N.M. & Jackson S.P. 2013. Deubiquitylating enzymes and DNA damage response pathways. Cell Biochemistry and Biophysics 67: 25-43.

Jentsch S., McGrath J.P., and Varshavsky A. 1987. The yeast DNA repair gene RAD6 encodes a ubiquitin-conjugating enzyme. Nature 329: 131–134.

Jin Q., Zhuang L., Lai B., Wang C., Li W., Dolan B., Lu Y., Wang Z., Zhao K., Peng W., Dent SYR and Ge K. 2014 Gcn5 and PCAF negatively regulate interferin-b production through HAT-independent inhibition of TBK1. EMPO reports

Kemper J.K., Xiao Z., Ponugoti B., Miao J., Fang S., Kanamaluru D. and Tsang S. et al. 2009. FXR acetylation is normally dynamically regulated by p300 and SIRT1 but constitutively elevated in metabolic disease states. Cell Metabolism 10: 392–404.

Kemper J.K., Choi S. and Kim D.H. 2013. Sirtuin 1 deacetylase: a key regulator of hepatic lipid metabolism. Vitamins and Hormones, volume 91, chapter 16.

Kapoor S. 2013. Usp22 and its evolving role in systemic carcinogenesis. Lung cancer 79 (2): 191-195.

Khorasanizadeh S. 2004. The nucleosome: from genomic organization to genomic regulation. Cell 116: 259-272.

Kim J., Hake S.B. and Roeder R.G. 2005. The human homolog of yeast BRE1 functions as a transcriptional coactivator through direct activator interactions. Molecular Cell. 20: 759-770.

Koehler C., Bonnet J., Stierle M., Romier C., Devys D. and Kieffer B. 2014. DNA binding by Sgf11 protein affects histone H2B deubiquitination by Spt-Ada-Gcn5 acetylatransferase (SAGA). The Journal of Biological Chemistry 289: 8989-8999

Kohler A., Pascual-Garcia P., Liopis A. and Zapater M. 2006. The mRNA export factor Sus1 is involved in Spt/ Ada/Gcn5 acetylatransferase-mediated H2B ubiquitinylation through its interaction with Ubp8 and Sgf11. Molecular Biology of the Cell 17 (10): 4228-4236.

Kohler A., Zimmerman E., Schneider M., Hurt E., Zheng N. 2010. Structural basis for assembly and activation of the heterotetrameric SAGA histone H2B deubiquitinase module. Cell 141: 606–617.

Koken M.H., Reynolds P., Jaspers-Dekker I., Prakash L., Prakash S., Bootsma D., and Hoeijmakers J.H. 1991. Structural and functional conservation of two human homologs of the yeast DNA repair gene RAD6. Proc. Natl. Acad. Sci. 88: 8865–8869.

Komander D., Clague M. J. and Urbe S. 2009. Breaking the chains: structure and function of the deubiquitinases. Nat. Rev. Mol. Cell Biol. 10: 550-563.

Komander D., Reyes-Turcu F. J. D., Odenwaelder P., Wilkinson K. D. and Barford D. 2009b. Molecular discrimination of structurally equivalent Lys63-linked and linear polyubiquitin chains. EMBO Report 10: 466-473.

Komander D., Rape M. 2012. The ubiquitin code. Annual Review of Biochemistry 81: 203–229.

Kornberg R.D. 1974. Chromatin structure: a repeating unit of histones and DNA. Science 184: 868-871.

Kouzarides T. 2007. Chromatin modifications and their function. Cell 128: 693-705.

Krebs A.R., Karmodiya K., Lindahl-Allen M., Struhl K. and Tora L. 2011. SAGA and ATAC histone acetyl transferase complexes regulate distinct sets of genes and ATAC defines a class of p300-independent enhancers. Molecular Cell 44: 410-423.

Kurshakova M.M., Krasnov A.N., Kopytova D.V., Shidlovskii Y.V., Nikolenko J.V., Nabirochkina E.N., Spehne D., Schultz P., Tora L., Georgieva S.G. 2007. SAGA and a novel Drosophila export complex anchor efficient transcription and mRNA export to NPC. EMBO Journal 26: 4956-4965.

Lang G., Bonnet J., Umlauf D., Karmodiya K., Koffler J., Stierle M., Devys D., Tora L. 2011. The tightly controlled deubiquitination activity of the human SAGA complex differentially modifies distinct gene regulatory elements. Molecular and Cellular Biology31 (18): 3734-3744.

Lee K.K., Florens L., Swanson S.K., Washburn M.P., and Workman J.L. 2005. The deubiquitylation activity of Ubp8 is dependent upon Sgf11 and its association with the SAGA complex. Molecular and Cellular Biology 25: 1173-1182.

Lee H., Kim M., Shin J., Park T., Chung H. and Baek K. 2006. The expression patterns of deubiquitinating enzymes, USP22 and Usp22. Gene expression patterns 6: 277-284.

Li X., Zhang S., Blander G., Tse J.G., Krieger M., Guarente L. 2007. SIRT1 deacetylates and positively regulates the nuclear receptor LXR. Molecular Cell 28(1): 91–106

Li J., Wang Z. and Li Y. 2012. Usp22 nuclear expression is significantly associated with progression and unfavorable clinical outcome in human esophageal squamous cell carcinoma. Journal of Cancer Research and Clinical Oncology 138: 1291-1297.

Li Z.H., Yu Y., DU C., Fu H., Wang J. and Tian Y. 2013. RNA interference-mediated USP22 gene silencing promotes human brain glioma apoptosis and induces cell cycle arrest. Oncology Letters 5 (4): 1290-1294.

Liang J., Zhang X., Xie S., Zhou X., Shi Q., Hu J., Wang W., Qi W. and Yu R. 2014. Ubiquitin-specific protease 22: a novel molecular biomarker in glioma prognosis and therapeutics. Medical Oncology 31: 899-905.

Lin Z., Yang H., Kong Q., Li J., Lee S., Gao B., Dong H., Wei J., Song J., Zhang D.D. and Fang D. 2012. Usp22 antagonizes p53 transcriptional activation by deubiquitinating Sirt1 to suppress cell apoptosis and is required for mouse embryonic development. Molecular Cell 46:1-11.

Ling S.B., Sun D.G., Tang B., Guo C., Zhang Y., Liang R. & Wang L.M. 2012. Knock-down of USP22 by small interfering RNA interference inhibits HepG2 cell proliferation and induces cell cycle arrest. Cellular and Molecular Biology (Noisy-le-grand) OL1803-1808.

Liu Y., Yang Y., Xu H. and Dong X. 2010. Implication of Usp22 in the regulation of Bmi-1, c-Myc, p16INK4a, p14ARF and cyclin D2 expression in primary colorectal carcinomas. Diagn. Mol. Pathol. 19 (4): 194-200.

Liu Y., Yang Y., Xu H. and Dong X. 2011. Aberrant expression of Usp22 is associated with liver metastasis and poor prognosis of colorectal cancer. Journal of Clinical Oncology 103: 283-289.

Lomb D.J., Laurent G. and Haigis M.C. 2010. Sirtuins regulate key aspects of lipid metabolism. Review. Biochimica and Biophysica Acta 1804:1652-1657.

Luger K., Mader A.W., Richmond R.K., Sargent D.F., and Richmond T.J. 1997. Crystal structure of the nucleosome core particle at 2.8 A resolution. Nature 389: 251–260.

Lv L., Xiao X.Y., Gu Z.H., Zeng F.Q., Huang L.Q. & Jiang G.S. 2011 Silencing USP22 by asymmetric structure of interfering RNA inhibits proliferation and induces cell cycle arrest in bladder cancer cells. Molecular and Cellular Biochemistry 346: 11-21.

Mao P., Meas R., Dorgan K.M. and Smerdon M.J. 2014. UV damage-induced RNA polymerase II stalling stimulates H2B deubiquitylation. Proceedings of the National Academy of Sciences of the United States of America.111 (35): 12811-12816.

Marquardt J.U. and Thorgeirsson S.S. 2014. Snapshot: Hepatocellular carcinoma. Cancer Cell 25. DOI http://dx.doi.org/10.1016/j.ccr.2014.04.002

Metzger M.B., Hristova V.A., Weissman A.M. 2012. HECT and RING finger families of E3 ubiquitin ligases at a glance. The Journal of Cellular Science 125: 531–537

Michalopoulos G.K., DeFrances M.C. 1997. Liver regeneration. Science 276 (5309): 60–66.

Mito Y., Henikoff J.G. and Henikoff S. 2005. Genome-scale profiling of histone H3.3 replacement patterns. Nature Genetics 37: 1090-1097.

Motta M.C., Divecha N., Lemieux M., Kamel C., Chen D., Gu W. et al. 2004. Mammalian SIRT1 represses forkhead transcription factors. Cell 116 (4): 551–63.

Nagy Z. and Tora L. 2007. Distinct GCN5/PCAF–containing complexes function as co-activators and are involved in transcription factor and global histone acetylation. Oncogene 26: 5341-5357.

Narlikar G.J., Fan H.Y. and Kingston R.E. 2002. Cooperation between complexes that regulate chromatin structure and transcription. Cell 108: 475-487.

Nickel B.E. and Davie J.R. 1989. Structure of polyubiquitinated histone H2A. Biochemistry 28: 964–968.

Nickel B.E., Allis C.D., and Davie J.R. 1987. Ubiquitinated histone H2B is preferentially located in transcriptionally active chromatin. Biochemistry 28: 958–963.

Nie Y., Erion D.M., Yuan Z., Dietrich M., Shulman G., Horvath T. and Gao Q. 2009. Stat3 inhibition of gluconeogenesis is down regulated by Sirt1. Nature Cell Biology 11 (4): 492-500.

Nijman S.M., Huang T.T., Dirac A.M., Brummelkamp T.R., Kerkhoven R.M., n D'Andrea A.D. and Bernards R. 2005. The deubiquitinating enzyme USP1 regulates the Fanconi anemia pathway. Molecular Cell 17: 331-339.

Nijman S.M., Luna-Vargas M.P., Velds A., Brummelkamp T.R., Dirac A.M., Sixma T.K. and Bernards R. 2005. A genomic and functional inventory of deubiquitinating enzymes. Cell 123: 773-786.

Ning J., Zhang J., Liu W., Lang Y., Xue Y. and Xu S. 2012. Overexpression of ubiquitin-specific protease 22 predicts poor survival in patients with early-stage non-small cell lung cancer. European Journal of Histochemistry 56 (4):e46.

Nisoli E., Tonello C., Cardile A., Cozzi V., Bracale R., Tedesco L. et al. 2005. Calorie restriction promotes mitochondrial biogenesis by inducing the expression of eNOS. Science. 310 (5746): 314–7

Nowak S.J. and Corces V.G. 2004. Phosphorylation of histone H3: A balancing act between chromosome condensation and transcriptional activation. Trends in Genetics 20: 214-220.

Osborne T.F. and Espenshade P.J. 2009. Evolutionary conservation and adaptation in the mechanism that regulates SREBP action: what a long, strange tRIP it's been. Genes and Development 23: 2578–2591.

Owen D.J., Ornaghi P., Yang J.C., Lowe N., Evans P.R., Ballario P., Neuhaus D., Filetici P., Travers A.A. 2000. The structural basis for the recognition of acetylated histone H4 by the bromodomain of histone acetyltransferase gcn5p. EMBO J 19: 6141-6149. 25.

Panzer O., Moitra V. and Sladen R.N. 2009. Pharmacology of sedative-analgestic agents: dexmedetomidine, remifentanil, ketamine, volatile anesthetics and the role of peripheral mu antagonists. Crit. Care Clin. 25 (3): 451-469.

Pascual-Garcia P., Govind C.K., Queralt E., Cuenca-Bono B., Llopis A., Chavez S., Hinnebusch A.G. and Rodriguez-Navarro S. 2008. Sus1 is recruited to coding regions and functions during transcription elongation in association with SAGA and TREX2. Genes Dev. 22: 2811-2822.

Peterson CL. 2002. Chromatin remodeling: Nucleosomes bulging at the seams. Current Biology- Cell 12: R245-R247.

Piao S., Liu Y., Hu J., Guo F., Ma J., Sun Y. & Zhang B. 2012. USP22 is useful as a novel molecular marker for predicting disease progression and patient prognosis of oral squamous cell carcinoma. PLoS One 7 e42540.

Piao S., Ma J., Wang W., Liu Y., Zhang M., Chen H., Guo F., Zhang B. and Guo F. 2013. Increased expression of Usp22 is associated with disease progression and patient prognosis of salivary duct carcinoma. Oral oncology 49: 796-801

Picard F., Kurtev M., Chung N., Topark-Ngarm A., Senawong T., Machado De Oliveira R. et al. 2004. Sirt1 promotes fat mobilization in white adipocytes by repressing PPAR-gamma. Nature 429 (6993): 771–776.

Pickart C.M. 2001. Mechanisms underlying ubiquitination. Annual Review of Biochemistry 70: 503–533.

Pijnappel W.W. and Timmers H.T. 2008. Dubbing SAGA unveils new epigenetic crosstalk. Mol. Cell. 29 (2): 152-154.

Ponugoti B., Kim D.H., Xiao Z., Smith Z., Miao J., Zang M. and Wu S.Y. et al. 2010. SIRT1 deacetylates and inhibits SREBP-1C activity in regulation of hepatic lipid metabolism. The Journal of Biological Chemistry 285: 33959–33970.

Price N.L., Gomes A.P., Ling A.J.Y., Duarte F.V., Martin-Montalvo A., North B.J., Agarwal B., Ye L., Ramadori G., Teodoro J.S., Hubbard B.P., Varela A.T., Davis J.G., Varamini B., Hafner A., Moaddel R., Rolo A.P., Coppari R., Palmeira C.M., De Cabo R., Baur J.A. and Sinclair D.A. 2012. Sirt1 is required for AMPK activation and the beneficial effects of resveratrol on mitochondrial function. Cell Metabolism 15: 675-690.

Purushotham A., Schug T.T., Xu Q., Surapureddi S., Guo X. and Li X. 2009. Hepatocyte-specific deletion of Sirt1 alters fatty acid metabolism and results in hepatic steatosis and inflammation. Cell Metabolism 9:327-338.

Reyes-Turcu F.E., Ventii K.H., Wilkinson K.D. 2009. Annual Review of Biochemistry 78: 363–397.

Riggins R.B., Schrecengost R.S., Guerrero M.S., Bouton A.H. 2007. Pathways to tamoxifen resistance. Cancer letters.256:1-24

Rodgers J.T., Lerin C., Haas W., Gygi S.P., Spiegelman B.M., Puigserver P. 2005. Nutrient control of glucose homeostasis through a complex of PGC-1alpha and SIRT1. Nature 434 (7029): 113–118.

Rodriguez-Navarro S., Fischer T., Luo M.J., Antunez O., Brettschneider S., Lechner J., Perez-Ortin J.E., Reed R., and Hurt E. 2004. Sus1, a functional component of the SAGA histone acetylase complex and the nuclear-pore associated mRNA machinery. Cell 116: 75-86.

Rodriguez-Navarro S. 2009. Insights into SAGA function during gene expression. EMBO reports 10 (8): 843-850

Samara N.L. and Wolberger C. 2011. A new chapter in the transcription SAGA. Current Opinion in Structural Biology 21: 764-774.

Samara N.L., Datta A.B., Berndsen C.E., Zhang X., Yao T., Cohen R.E. and Wolberger C. 2010. Structural insights into the assembly and function of the SAGA deubiquitinating module. Science 328 (5981): 1025-1029.

Satija Y.K., Bhardwaj A. and Das S. 2013. A portrayal of E3 ubiquitin ligases and deubiquitylases in cancer. International Journal of Cancer 133 (12): 2759-2768.

Schenk S., McCurdy C.E., Philp A., Chen M.Z., Holliday M.J., Bandyopadhyay G.K., Osborn O., Baar K. and Olefsky J.M. 2013. Sirt1 enhances skeletal muscle insulin sensitivity in mice during caloric restriction. The Journal of Clinical Investigation 11 (121): 4281-4286.

Schrecengost R.S., Dean J.L., Goodwin J.F., Schiewer M.J., Urban M.W., Stanek T.J., Sussman R.T., Hicks J.L., Birbe R.C., Draganova-Tacheva R.A., Visakorpi T., DeMarzo A.M., McMahon S.B. and Knusden K.E. 2014. USP22 regulates oncogenic signaling to drive lethal cancer progression. Cancer Research 74 (1): 272-286.

Schreiber S.L. and Bernstein B.E. 2002. Signaling network model of chromatin. Cell 111: 771-778.

Shukla A., Bajwa P. and Bhaumik S.R. 2006. SAGA-associated Sgf73p facilitiates formation of the preinitiation complex assembly at the promoters either in a HAT –dependent or independent manner in vivo. Nucleic Acids Research 34 (21): 6225-6232.

Shukla A., Stanojevenic N., Duan Z., Sen P. and Bhaumik S.R. 2006. Ubp8, a histone deubiquitinase whose association with SAGA is mediated by Sgf11p, differentially regulates lysine 4 methylation of histone H3 in vivo. Molecular and Cellular Biology 26 (9): 3339-3352

Sigismund S., Polo S., Di Fiore P. P. 2004. Signaling through monoubiquitination. Current Topics in Microbiology and Immunology. 286: 149–185

Singhal S., Taylor M.C. & Baker R.T. 2008 Deubiquitylating enzymes and disease. BMC Biochemistry 9 Suppl 1 S3.

Sowa M.E., Bennett E.J., Gygi S.P. & Harper J.W. 2009. Defining the human deubiquitinating enzyme interaction landscape. Cell 138: 389-403.

Strahl B.D. and Allis C.D. 2000. The language of covalent histone modifications. Nature 403: 41-45.

Sterner D.E., Grant P.A., Roberts S.M., Duggan L.J., Belotserkovskaya R., Pacella L.A., Winston F., Workman J.L., Berger S.L. 1999. Functional organization of the yeast SAGA complex: distinct components involved in structural integrity, nucleosome acetylation, and TATA-binding protein interaction. Molecular and Cellular Biology 19: 86-98.

Suliburk J.W., Gonzalez E.A., Kennison S.D., Helmer K.S. and Mercer D.W. 2005. Differential effects of anesthetics on endotoxin-induced liver injury. Journal of Trauma and Acute Care Surgery 58 (4): 711-716.

Sun Z. and Allis C.D. 2002. Ubiquitylation of histone H2B regulates H3 methylation and gene silencing in yeast. Nature 418: 104-108.

Sussman R.T., Stanek T.J., Esteso P., Gearhart J.D., Knusden K.E. and McMahon S.B. 2013. The epigenetic modifier ubiquitin-specific protease 22 (Usp22) regulates embryonic stem cell differentiation via transcriptional repression of Sex-determining region Y-box2 (Sox2). The Journal of Biological Chemistry 288: 24234-24246.

Thompson N.L., Mead J.E., Braun L. 1986. Sequential proto-oncogene expression during rat liver regeneration. Cancer Research. 46(6): 3111–3117.

Tontonoz P. and Spiegelman B.M. 2008. Fat and beyond: the diverse biology of PPARgamma. Annual Review of Biochemistry 77: 289–312.

Trujilllo K.M. and Osley M.A. 2012. A role for H2B ubiquitylation in DNA replication. Molecular Cell 48: 734-746.

Tsukiyama T., Daniel C., Tamkun J. and Wu C. 1995. ISWI, a member of the SWI2/SNF2 ATPase family, encodes the 140 kDa subunit of the nucleosome remodeling factor. Cell 83: 1021-1026.

Turner B.M. 2000. Histone acetylation and an epigenetic code. Bioessays 22: 836-845.

Varga-Weisz P.D., Wilm M., Bonte E., Dumas K., Mann M. and Becker P.B. 1997. Chromatin-remodeling factor CHRAC contains the ATPases ISWI and topoisomerase II. Nature 388: 598-602.

Walker A.K., Yang F., Jiang K., Ji J.Y., Watts J.L., Purushotham A. and Boss O. et al. 2010. Conserved role of SIRT1 orthologs in fasting-dependent inhibition of the lipid/cholesterol regulator SREBP. Genes and Development 24: 1403–1417.

Wang Y., Wysocka J., Sayegh J., Lee Y.H., Perlin J.R., Leonelli L., Sonbuchner L.S., McDonald C.H., Cook R.G., Dou Y. et al. 2004. Human PAD4 regulates histone arginine methylation levels via dmethylination. Science 306: 279-283.

Wang X., Gu J., Ihara H., Miyoshi E., Honke K., Taniguchi N. 2006. Core fucosylation regulates epidermal growth factor receptor-mediated intracellular signaling. The Journal of Biological Chemistry 281: 2572–2577.

Wang X., Herr R.A., Chua W.J., Lybarger L., Wiertz E.J., Hansen T.H. 2007. "Ubiquitination of serine, threonine, or lysine residues on the cytoplasmic tail can induce ERAD of MHC-I by viral E3 ligase mK3". The Journal of Cellular Biology 177 (4): 613–24.

Wang H., Li Y., Chen J., Yuan S., Wang L., Liang J., Yao Q., Li N., Bian J., Fan J., Yi J. and Ling R. 2013. Prognostic significance of Usp22 as an oncogene in papillary thyroid carcinoma. Tumor Biology 34: 1635-1639.

Wang L. and Dent S. 2014. Functions of SAGA in development and disease. Epigenetics 6 (3): 329-33.

Weake V.M., Lee K.K., Guelman S., Lin C.H., Seidel C., Abmayr S.M. and Workman J.L. 2008. SAGA-mediated H2B deubiquitination controls the development of neuronal connectivity in the Drosophila visual system. EMBO 27 (2): 394-405.

West M.H. and Bonner W.M. 1980. Histone 2B can be modified by the attachment of ubiquitin. Nucleic Acids Research .8: 4671– 4680.

Wolfer A., Wittner B.S., Irimia D., Flavin R.J., Lupien M., Gunawardane R.N. et al. 2010. MYC regulation of a "poor-prognosis" metastatic cancer cell state. Proceedings of the National Academy of Sciences of the United States of America. 107: 3698-703.

Wood A., Krogan N.J., Dover J., Schneider J., Heidt J., Boateng M.A., Dean K., Golshani A., Zhang Y., Greenblatt J.F. et al. 2003. Bre1, an E3 ubiquitin ligase required for recruitment and substrate selection of Rad6 at a promoter. Molecular Cell 11: 267-274.

Xiao T., Kao C., Krogan N.J., Sun Z., Greenblatt J.F., Osley M.A. and Strahl BD. 2005. Histone H2B ubiquitylation is associated with elongating RNA Polymerase II. Molecular and Cellular Biology: 637-651.

Xiong J., Wang Y., Gong Z., Liu J. and Li W. 2014. Identification of a functional nuclear localization with the human Usp22 protein. Biochemical and Biophysical Research Communication 449 (1):14-18.

Yang W., Zhang X. and Lin H. 2010. Emerging role of Lys-63 ubiquitination in protein kinase and phosphatase activation and cancer development. Oncogene 29 (32):4493-4503.

Yang D., Cui B., Sun L., Zheng H., Huang Q., Tong J. and Zhang Q. 2011. The co-expression of Usp22 and Bmi-1 may promote cancer progression and therapy failure in gastric carcinoma. Cell Biochem Physic 61: 703-710.

Yang M., Liu Y.D., Wang Y.Y., Liu T.B., Ge T.T. and Lou G. 2014. Ubiquitin-specific protease 22: a novel molecular biomarker in cervical cancer prognosis and therapeutics. Tumor Biol. 35 (2): 929-934.

Zhang H., Roberts D.N. and Cairns BR. 2005. Genome-wide dynamics of Htz1, a histone H2A variant that poises repressed/basal promoters for activation through histone loss. Cell 123: 219-231.

Zhang X., Varthi M., Sykes S.M., Phillips C., Warzecha C., Zhu W., Wyce A., Thorne A.W., Berger S.L., and McMahon S.B. 2008. The putative cancer stem cell marker Usp22 is as subunit of the human Saga complex required for activated transcription and cell-cycle progression. Molecular Cell 29: 102-111.

Zhao Y., Lang G., Ito S., Bonnet J., Metzger E., Sawatsubashi S., Suzuki E., Le Guezennec X., Stunnenberg H.G., Krasnov A., Georgieva S.G., Schule R., Takeyama K., Kato S., Tora L. and Devys D. 2008. A TFTC/STAGA module mediates histone H2A and H2B deubiquitination, coactivates nuclear receptors, and counteracts heterochromatin silencing. Molecular Cell 29: 92-101.

Zhang F. and Yu X. 2011. WAC, a functional partner of RNF20/40, regulates histone H2B ubiquitination and gene transcription. Mol Cell 41: 384-397.

Zhu B., Zheng Y., Pham A.D., Mandal S.S., Erdjument-Bromage H., Tempst P. and Reinberg D. 2005. Monoubiquitination of human histone H2B: The factors involved and their roles in HOX gene regulation. Mol. Cell 20: 601-611.